U.S. DEPARTMENT OF ENERGY

PNNL-21842

Prepared for the U.S. Department of Energy
under Contract DE-AC05-76RL01830

Bonneville Project: CFD of the Spillway Tailrace

CL Rakowski
JA Serkowski
MC Richmond
PDJ Romero-Gomez

November 2012

Pacific Northwest NATIONAL LABORATORY

Proudly Operated by Battelle Since 1965

DISCLAIMER

PACIFIC NORTHWEST NATIONAL LABORATORY
operated by
BATTELLE
for the
UNITED STATES DEPARTMENT OF ENERGY
under Contract DE-AC05-76RL01830

Printed in the United States of America

Available to DOE and DOE contractors from the
Office of Scientific and Technical Information,
P.O. Box 62, Oak Ridge, TN 37831-0062;
ph: (865) 576-8401
fax: (865) 576-5728
email: reports@adonis.osti.gov

Available to the public from the National Technical Information Service
5301 Shawnee Rd., Alexandria, VA 22312
ph: (800) 553-NTIS (6847)
email: orders@ntis.gov <http://www.ntis.gov/about/form.aspx>
Online ordering: http://www.ntis.gov

(8/2010)

PNNL-21842

Bonneville Project: CFD of the Spillway Tailrace

CL Rakowski
JA Serkowski
MC Richmond
PDJ Romero-Gomez

November 2012

Prepared for
the U.S. Department of Energy
under Contract DE-AC05-76RL01830

Pacific Northwest National Laboratory
Richland, Washington 99352

Summary

U.S. Army Corps of Engineers, Portland District (CENWP) operates the Bonneville Lock and Dam Project on the Columbia River. High spill discharges that occurred during 2011 moved a large volume of rock from downstream of the spillway apron to the stilling basin and apron. Although 400 cubic yards of rocks were removed from the stilling basin, there are still large volumes of rock downstream of the apron that could, under certain flow conditions, move upstream into the stilling basin. CENWP is investigating operational changes that could be implemented to minimize future movement of rock into the stilling basin. A key analysis tool to develop these operational changes is a computational fluid dynamics (CFD) model of the spillway.

A free-surface CFD model of the Bonneville spillway tailrace was developed and applied for four discharge scenarios. These scenarios looked at the impact of discharge volume and distribution on tailrace hydraulics. The simulation results showed that areas of upstream flow existed near the river bed downstream of the apron, on the apron, and within the stilling basin for all discharges. For spill discharges of 300 kcfs, the cross-stream and downstream extent of the recirculation zones along Cascade and Bradford islands was very dependent on the spill pattern. The center-loaded pattern had much larger recirculation zones than the flat or bi-modal pattern. The lower discharge (200 kcfs) with a flat pattern had a very large recirculation zone that extended halfway across the channel near the river bed.

A single scenario (300 kcfs of discharge in a relatively flat spill pattern) was further interrogated using Lagrangian particle tracking. The tracked particles (with size and mass) showed the upstream movement of sediments onto the concrete apron and against the vertical wall between the apron and the stilling basin from seed locations downstream of the apron and on the apron.

Abbreviations and Acronyms

3D	three-dimensional
ADV	acoustic Doppler velocimeter
B2	Bonneville Powerhouse 2
CAD	computer-aided design
CENWP	U.S. Army Corps of Engineers, Portland District
cfs	cubic feet per second
CFD	computational fluid dynamics
ft/s	feet per second
ERDC	Engineer Research and Development Center, Vicksburg, Mississippi
GIS	geographic information system
HRIC	high resolution interface capturing
kcfs	thousand cubic feet per second
NAVD29	North American Vertical Datum of 1929
PNNL	Pacific Northwest National Laboratory
RANS	Reynolds-averaged Navier-Stokes
s	second
STL	stereolithography
STS	standard traveling screen
TWE	tailwater elevation
UD	upwind differencing
USACE	U.S. Army Corps of Engineers
vmag	velocity magnitude
VOF	volume of fluid

Acknowledgments

Financial support for this study was provided by the U.S. Army Corps of Engineers (USACE) under MIPR W66QK11794377(A1). The authors would like to thank Laurie Ebner (USACE, Portland District) for the discussions, support, and insight that improved this study, and Bill Perkins for comments, which improved this report. A portion of the research was performed using PNNL Institutional Computing at Pacific Northwest National Laboratory.

Contents

Figures

Tables

1.0 Introduction

U.S. Army Corps of Engineers, Portland District (CENWP) operates the Bonneville Lock and Dam Project (Figures 1.1 and 1.2) on the Columbia River. High spill discharges that occurred during 2011 moved a large volume of rock from downstream of the spillway apron to the stilling basin and apron. A contract was executed to remove the rocks from the stilling basin to prevent future damage due to ball milling caused by rocks churning in the stilling basin (Figure 1.3). Although 400 cubic yards of rocks were removed from the stilling basin there are still large volumes of rock downstream of the apron that could, under certain flow conditions, move upstream into the stilling basin. CENWP is investigating operational changes that could be implemented to minimize future movement of rock into the stilling basin. A key analysis tool to develop these operational changes is a computational fluid dynamics (CFD) model of the spillway.

In previous work, Pacific Northwest National Laboratory (PNNL) researchers modeled the Bonneville tailrace with a transient, free surface CFD model (Rakowski et al. 2010). The area of interest of this earlier work was not focused on the stilling basin and the grid was too coarse for this effort. PNNL had to perform the following improvements/changes to the old spillway model: new geometry was created in computer-aided design (CAD) software based on the most recent bathymetric surveys and detailed drawings of the spillway bays, fishways, stilling basin, baffle blocks and apron.

The objectives of this study were as follows:

- Create a new CAD geometry and CFD model based on the most current bathymetric data.
- Run the CFD model for several spillway flow distributions.
- Analyze CFD results for potential pathways for large sediments to move into the stilling basin for the different spill patterns.

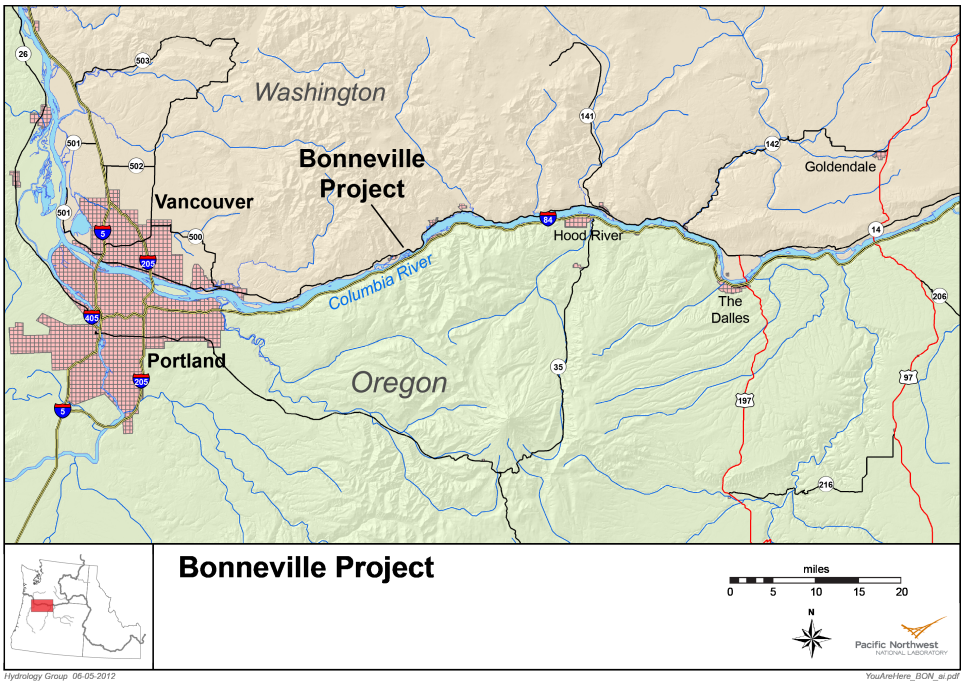

Figure 1.1. Location of the Bonneville Project

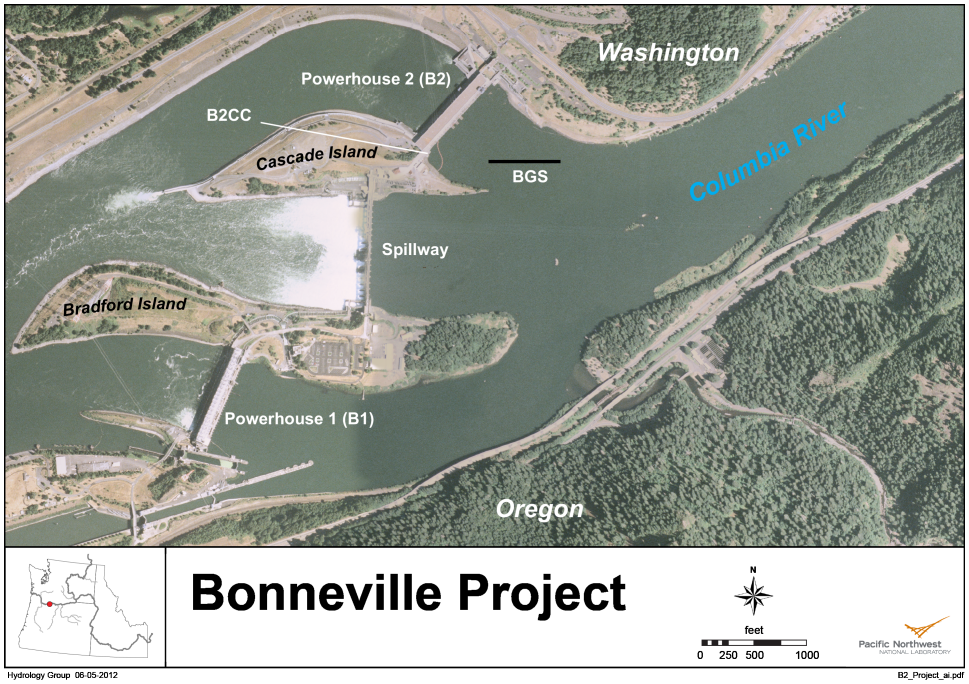

Figure 1.2. Detail of the Bonneville Project. Flow is from right to left.

Figure 1.3. Rocks removed from the spillway stilling basin in March of 2012.

2.0 Methods

The methods described below include the modeling approach, geometry development, mesh development, model validation, operational scenarios, and analysis of results. It should be noted that a mix of English and metric units co-exist in this document. Many features of the Bonneville Project are referenced by names such as the 7-ft deflector; most scientists and engineers who work at the project have an intuitive knowledge of the elevations in feet and discharge in cubic feet per second (cfs). However, the CFD work is based on metric units.

2.1 Geometry Development for Spillway Structures and Tailrace Bathymetry

The geometry model for the Bonneville Dam spillway modeling effort consists of two parts, the engineered structure and the tailrace channel bathymetry. These parts are distinguished by their sources of data and method of construction. The engineered structure, which includes the spillway ogee, flow deflectors, piers, baffle blocks, and fishway entrances (Figure 2.1), was built using a computer-aided design (CAD) application (SolidWorks^{TM} from Dassault Systèmes) from drawings provided by the CENWP (Table 2.1). Although provided as digitized image files, the drawings did not contain any measurements that could be automatically transferred to the CAD system, so all features were recreated manually using the indicated dimensions. The images served as underlays in the CAD for verification and, in some cases, to estimate dimensions not explicitly shown on the drawings. The resulting CAD model was exported to Parasolid format for CFD-model mesh generation.

Table 2.1. Construction drawings used for geometry model.

Structure	Documents
Ogee	M-5-12/67
Piers	M-5-12/67
Deflectors	BDF-2-49/3, BDD-2-7/1
Fishways	M-5-8/9, M-5-12/64
Stilling Basin	M-5-12/67, BDF-0-32/3

The river-channel bathymetry was modeled using a geographic information system (GIS) application (ArcGIS^{TM} version 9.3.1 from ESRI, Inc.) from bathymetric survey and aerial photography data (Figure 2.2). The bathymetric surface extends from, and includes, the concrete apron immediately downstream of the stilling basin to the western tip of Cascade Island and is bounded by a shore elevation of about 20 ft. Although the concrete apron is an engineered structure, it was included with the bathymetry surface because precise drawings of its current configuration were not available. While the bathymetric survey data provided the majority of the information necessary to create surface, additional contour and control lines were manually digitized to improve the interpolation in areas where data were lacking and to provide proper connection to the CAD model. The GIS application interpolated the elevation data onto a square-element mesh divided, to reduce file size, into two resolution regions. In the upstream 600 ft of the domain, where a high-resolution multi-beam survey was conducted in October 2011, the mesh spacing was 1.64 ft (0.5 m), while in the remainder of the channel, where data were sparser, spac-

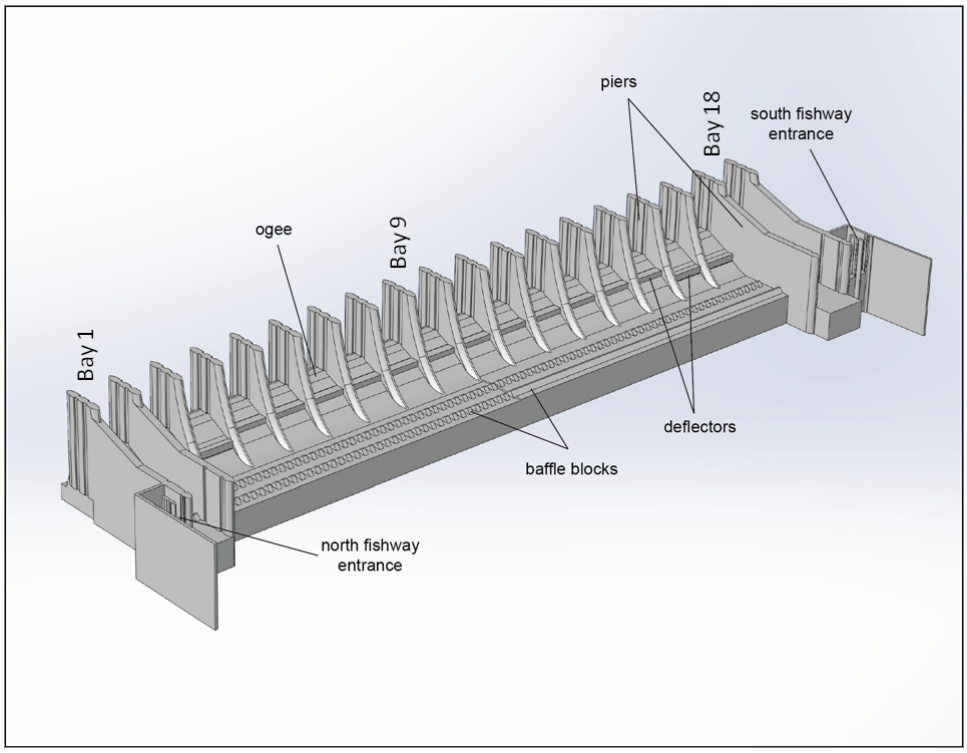

Figure 2.1. Engineered structures

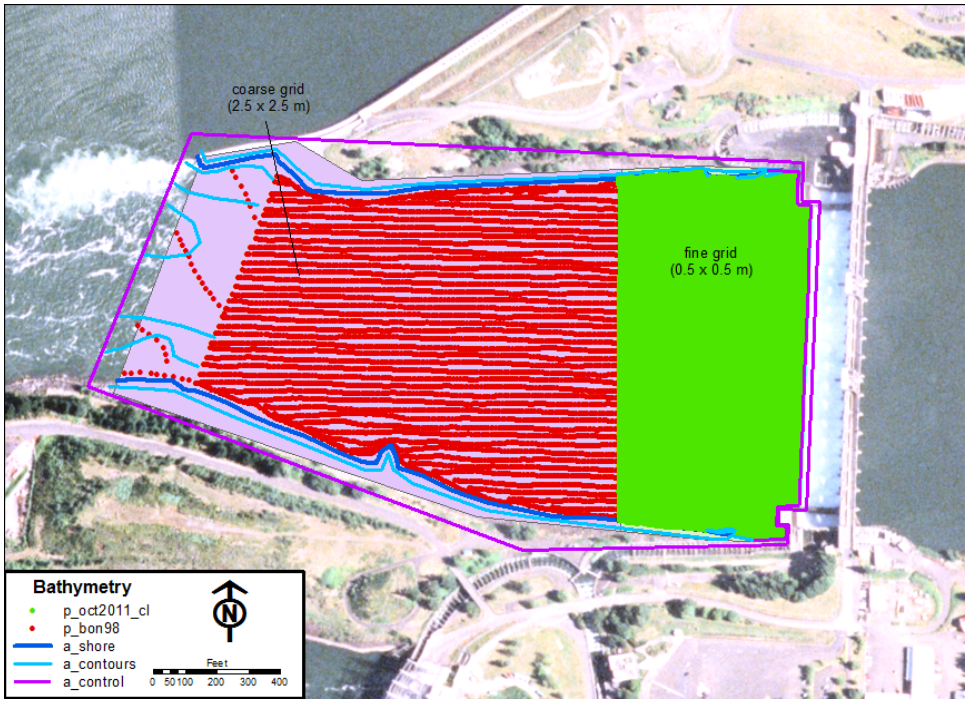

Figure 2.2. Data sets used to create bathymetric surface. The underlying lavender polygon is the extent of the CFD model.

ing was 8.20 ft (2.5 m). The surface grid was exported to stereolithographic (STL) format for CFD-model mesh generation.

2.2 Geometry Integration

Structure and tailrace bathymetry were translated onto a common coordinate system. In this case, the bathymetry was in the geo-referenced coordinate system Washington South State Plane coordinate system, NAD datum of 1983 (NAD83) meters, vertical datum NGVD29 meters, the concrete on its own coordinate system which had the same angle relative to the river as the geo-referenced coordinates. The lateral offset for the spillway coordinate system was: X = +387602.7 m, Y = +35430.8 m. The bathymetric surface was translated to the spillway coordinate system as it is required that the spatial coordinate values to be less than 10e5 for STAR-CCM+.

After the two surface meshes were in the same coordinate system (Figure 2.3), the cells that would be the interface between the meshes were removed and tools within STAR-CCM+ used to make a single, continuous surface for the whole domain. Boundaries were separated for each of the bays, the bathymetry, top, and features of the stilling basin. Different mesh resolutions were assigned as needed. For example, a higher-resolution mesh was defined for the spillway bay inflows.

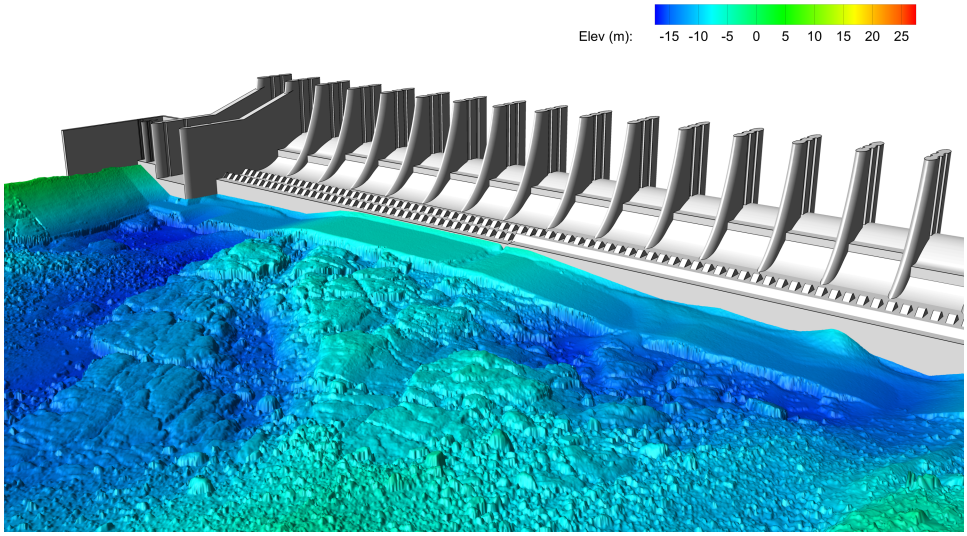

Figure 2.3. Spillway structure integrated with bathymetry. View is looking obliquely upstream; north side of the spillway is on the left.

2.3 Computational Mesh

The final computational mesh had 23M cells. The areas near the spillway ogee, piers, and baffle blocks were well resolved (Figure 2.4). The target surface-mesh resolution on the baffle blocks was 0.25 m and 0.4 m elsewhere in the stilling basin. Downstream bathymetry predominantly had a surface-mesh resolution of 0.4 m. STAR-CCM+ meshing parameters were set to have increased vertical resolution near the expected water surface elevation interface and a 4-cell

extrusion layer off all surfaces (Figure 2.5). It was necessary to have increased vertical and horizontal resolution in the downstream air-water interface elevations for the solution to develop a well-defined interface. Cells that are larger in the horizontal plane tend to have more smeared interfaces.

Although the vertical face of each inlet bay was a single boundary, the created volume mesh was split on each boundary at an appropriate elevation for the gate opening (note red and gold coloration in Figure 2.4). The downstream outlet was split above the water surface elevation and the lower boundary had a hydrostatic boundary with the specified water surface elevation applied; the upper outlet boundary was restricted to having only air flow.

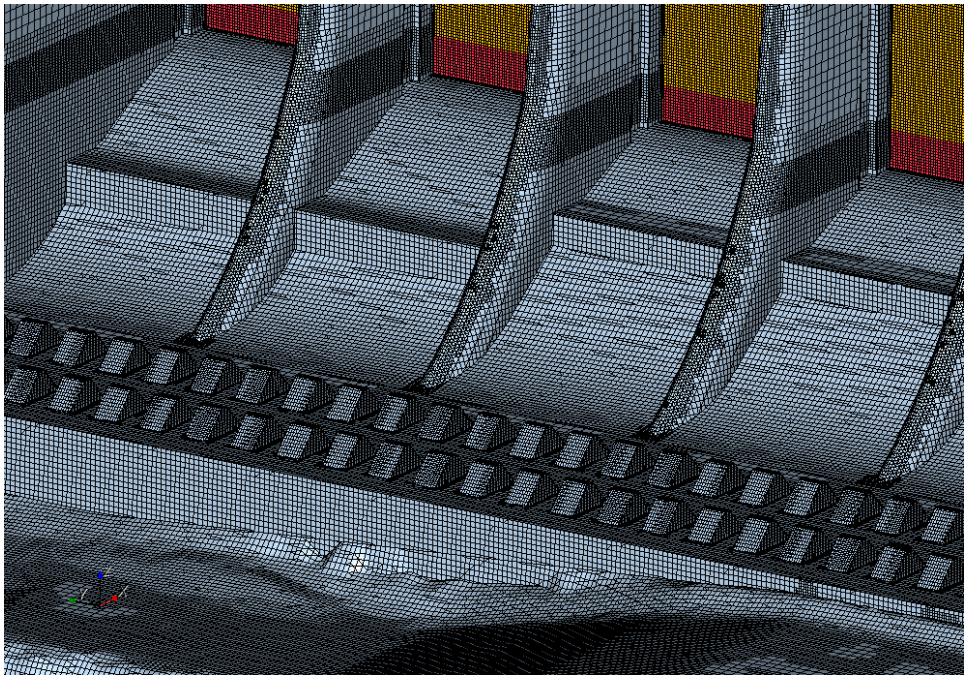

Figure 2.4. Detail of surface mesh on the spillway structure and bathymetry. View is of Bays 2, 3, 4, and 5 from left to right, respectively, and looking toward the north. Note deflectors at elevation 7 ft in Bays 2 and 3, deflectors at elevation 14 ft in Bays 4 and 5.

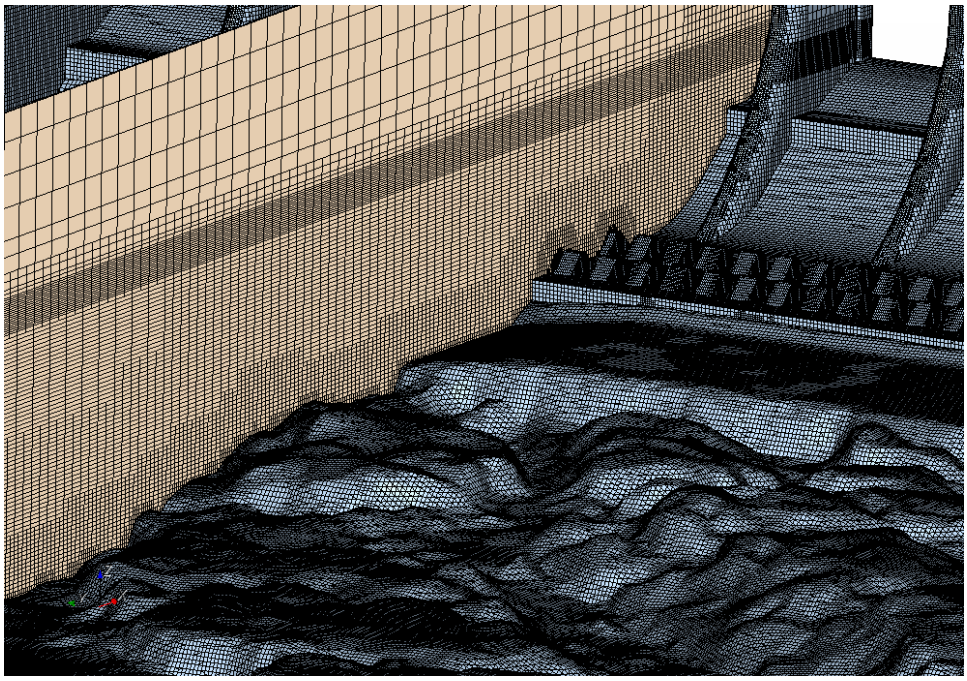

Figure 2.5. Detail vertical cut of the mesh near the spillway structure and bathymetry. Vertical cut is in Bay 4. Note increased resolution near the inflow boundaries and the expected water surface elevation.

2.4 Modeling Approach

STAR-CCM+ (ADAPCO, Computational Dynamics Limited 2012) was used to solve the Reynolds-averaged Navier-Stokes equations for a transient model of segregated isothermal flow; it was run second order in space, first order in time. The inflow conditions were steady-state velocity and a hydrostatic pressure boundary was used at the outlet. This study used the volume-of-fluid (VOF) multi-phase flow capabilities of the STAR-CCM+ code to simulate the air/water interface.

The k-ε turbulence closure was used. The high-resolution interface capturing (HRIC) scheme was used for air-water interfaces. For Courant numbers less than 1.0, a purely HRIC scheme was used, for Courant numbers between 1 and 5 a blended HRIC and upwind differencing (UD) scheme was used, and for interface areas with Courant numbers greater than 5.0, only the UD scheme was used. The average Courant number was monitored on the air-water interface, and the time step chosen such that the average Courant number on that interface was between 0.1 and 1, as recommended. The time step used was 0.15 s, and average Courant number on the air/water interface was approximately 0.7.

2.5 Modeled Scenarios

This study simulated discharge scenarios (Table 2.2) selected from the suite of physical model runs. Model run naming convention was taken from the CENWP's Engineer Research and Development Center (ERDC), Vicksburg, MS trip report [(a)] for consistency.

Run 3 represented a scenario that had high spill with a very flat pattern that was expected to move rocks. Run 1 was a lower spill discharge and no expected rock movement. Run 4 had high spill, but a more shaped spill pattern with the largest gate openings in the middle of the river. Run 6 had a bimodal spill distribution with smaller gate openings in the middle and on the edges of the spillway.

Results from the scenarios were visualized in three ways:

- Streamlines were seeded in nine locations in each of the spillway bays. These give a general sense of the overall flow pattern. The streamlines were colored by the downstream component of the velocity. These clearly show the extent of the lateral recirculation along the shores of Bradford and Cascade islands. It also shows any recirculation across the apron and into the stilling basin.

- Streamlines were seeded 0.5 m above the bathymetry downstream of the apron (Figure 2.6). These streamlines show the near-bed velocities and general flow patterns lower in the water column.

(a) CENWP. Trip Report - ERDC 1:55 Scale Bonneville Spillway General Model site visit (for rock removal work) March 11-16, 2012

Table 2.2. Specified operations for model scenarios. Flows in kcfs, tailwater elevation (TWE) in feet.

Scenario	Bay 1	2	3	4	5	6	7	8	9	10	11	12	13	14	15	16	17	18	TWE
Run 3 300kcfs	10.5	15.9	17.6	16.8	17.6	17.6	17.6	17.6	17.6	17.6	17.6	17.6	17.6	17.6	17.6	17.6	16.8	10.5	30
Run 1 200 kcfs	8.5	11.5	11.5	11.5	11.5	11.5	11.5	11.5	11.5	11.5	11.5	11.5	11.5	11.5	11.5	11.5	11.5	8.5	25
Run 4 300 kcfs	8.5	10.5	12.4	17.6	19.3	19.3	20.9	20.9	22.5	20.9	19.3	19.3	19.3	19.3	17.6	12.4	10.5	8.5	30
Run 6 300 kcfs	10.5	17.6	20.9	20.9	17.6	15.9	15.9	15.9	14.2	14.2	15.9	15.9	15.9	17.6	20.9	20.9	17.6	10.5	30

- A graphic was created of the water surface elevation. This clearly shows the location of standing waves and provides check of the overall flow pattern.

Although seeding streamlines near the river bed is an improvement over seeding streamlines in the spillway inflows, it does not capture the flow behavior at the bed that are responsible for mobilizing and moving the larger-clast sediments.

2.6 Particle Tracking and Rock Movement

The streamlines discussed above show the overall flow patterns and do not focus on the near-bed flows. To provide a qualitative understanding of the near-bed flows, the rock movement was modeled with the Lagrangian multiphase modeling capabilities in STAR-CCM+. Rocks were represented as solid spherical particles upon which the following surface and body forces act: drag (Schiller-Naumann formulation), pressure (pressure gradients from continuous phase), virtual mass ($C_{vm} = 0.5$), gravity, and lift ($C_L = 0.75$, Ecauriaza and Sotiropoulos (2011)). The spherical particles were of uniform diameter equal to 0.1 m and of density equal to 1350 kg/m^3, which is approximately one half of the actual rock density. This lower density was used to reduce the simulation time required to move the particles longer distances for this capability demonstration. Lagrangian particles do not interact with each other; neither do they affect the flow through which they travel (no coupling) and they rebound on all solid boundaries with normal and tangential restitution coefficients of 0.9 and 0.2, respectively.

Scenarios were simulated to test discharge and seeding configurations, all instances based on the high spill, flat pattern (Run 3, Table 2.2); results are described Section 3.2.2. In the first scenario (S1), the impact of the temporal flow formulation (frozen solution or transient solution) on the particle tracks was evaluated by seeding two arrays of 400 particles (20 x 20) roughly located 60 m downstream from bays 3 and 16 (Figure 2.7, top). The particle tracks were calculated over 300 seconds using the simulated flow results from a single time step (frozen flow solution) as well as for a transient flow solution. In second (S2) and third (S3) particle tracking scenarios, two additional seed configurations were tested under a transient flow solution with particles initially located on the concrete apron downstream of the stilling basin. The S2 scenario had the particles seeded in a rectangular array (15 x 15) roughly downstream from bays 9 and 10 (Figure 2.7, middle), whereas the S3 consisted of seven line-like arrangements, 15 m in length, as shown in Figure 2.7, bottom.

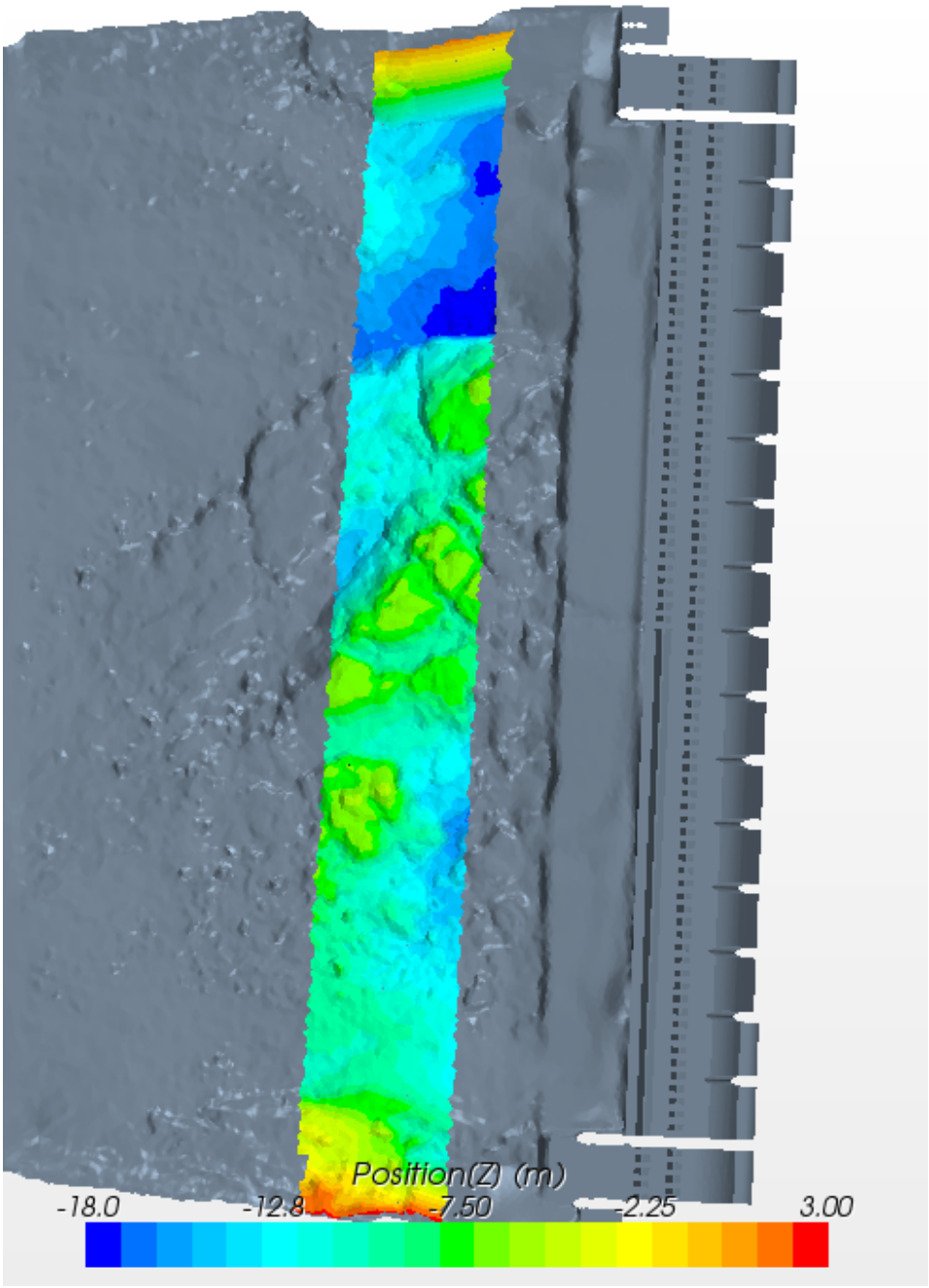

Figure 2.6. Surface used for seeds 0.5 m off the river bed. River bathymetry was translated by 0.5 m, and a section downstream of the stilling basin used as the source surface for streamline seeds.

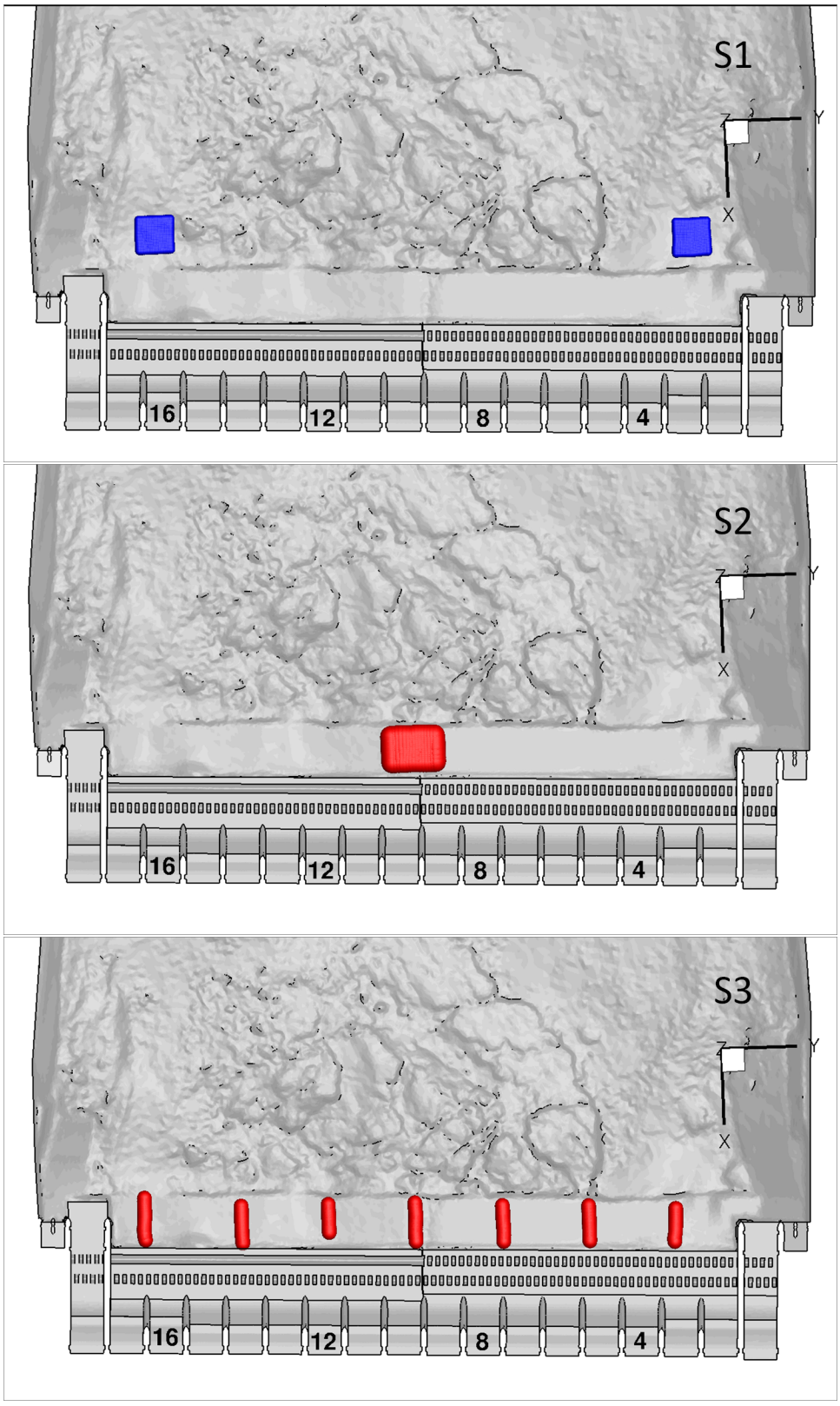

Figure 2.7. Initial seed locations for particle tracking for the three rock movement scenarios.

3.0 Results and Discussion

These simulation results are to be used to increase the understanding of the flow patterns downstream of the Bonneville spillway. Reduce-scale physical modeling has been done for these flow patterns; however, it was difficult to observe the movement of "rocks" while water was flowing in the physical model. It was also noted in the CENWP's ERDC model trip report [(a)] that the gravel used to represent the rocks in the physical model moved sooner than was observed at the prototype. Note that the naming convention for the CFD scenarios is consistent with that of the physical model studies.

3.1 1:40 Scale Bonneville Spillway Section Physical Model

No validation data exist for the spillway tailrace with large spill discharges. Qualitative data of jet behavior was collected in a 1:40 reduced-scale sectional physical model for the 14-ft flow deflectors for a range of discharges and tailwater elevations. [(b)] Figure 3.1 shows the expected behavior of spillway flow jet as a function of tailwater elevation and spillway discharges derived from the physical model study. As a secondary *y*-axis, the tailwater elevation is converted to jet submergence.

For the 300-kcfs spill runs (Runs 3, 4, and 6), the tailwater elevation was 30 ft. For a deflector elevation of 14 ft, the jet submergence was 16 ft. For the 7-ft deflectors, jet submergence was 23 ft. Figure 3.1 indicates that an undulating surface jet was expected for discharges between about 6 kcfs and 14 kcfs for the 14-ft deflector. Using the submergence of 23 ft for the 7-ft deflector, a submerged jump was expected for discharges up to about 10 kcfs, then an unstable surface jet for higher discharges. The CFD simulations of the spillway jets entering the tailrace had results consistent with expected behavior from the physical model study. Bays 1 and 18 were confined by concrete walls, necessitating lower discharges through these bays than the other bays; a submerged jump was modeled for all runs in Bays 1 and 18.

Figures 3.2 through 3.5 show vertical slices of the upstream component of the water velocities (in m/s) for Bays 9, 16, and 17. The velocity component is the *x*-component of the velocity vector which is very close to the streamwise velocity. The slices are for four levels of submergence and a suite of velocities; see Table 3.1 for details. The modeled inflow jet behavior was very consistent with that modeled in the physical model.

(a) CENWP Trip Report - ERDC 1:55 Scale Bonneville Spillway General Model site visit (for rock removal work) March 11-16, 2012

(b) CEWES-CR-F (1110-2-1402b) April 7, 1999. Data Report, Modified Bonneville Deflector, Bonnville Spillway Section Model

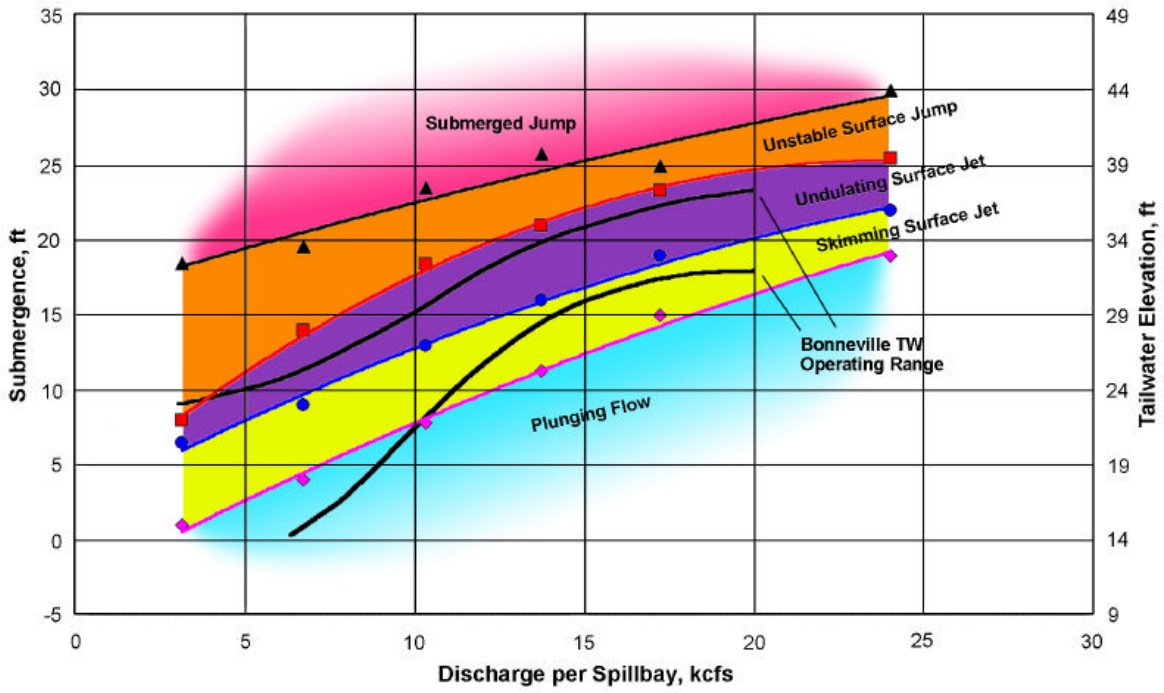

Figure 3.1. Expected jet flow characteristics for the 14-ft deflectors from 1:40 sectional physical model study.

Table 3.1. Spillway jet characteristics. Submergence was calculated for the 7-ft deflector bays.

Run	Bay	Submergence (ft)	Bay Inflow (kcfs)	CFD Behavior
6	Bay 16	23	20.9	Surface jet
3	Bay 16		17.6	Surface jet
4	Bay 16		12.4	Surface jump
4	Bay 17		10.5	Surface jump
1	Bay 16	18	11.5	Unstable surface jump
4	Bay 9	16	22.5	Skimming surface jet
3	Bay 9		17.6	Skimming surface jet
6	Bay 9		14.2	Undulating surface jet
1	Bay 9	11	11.5	Skimming surface jet

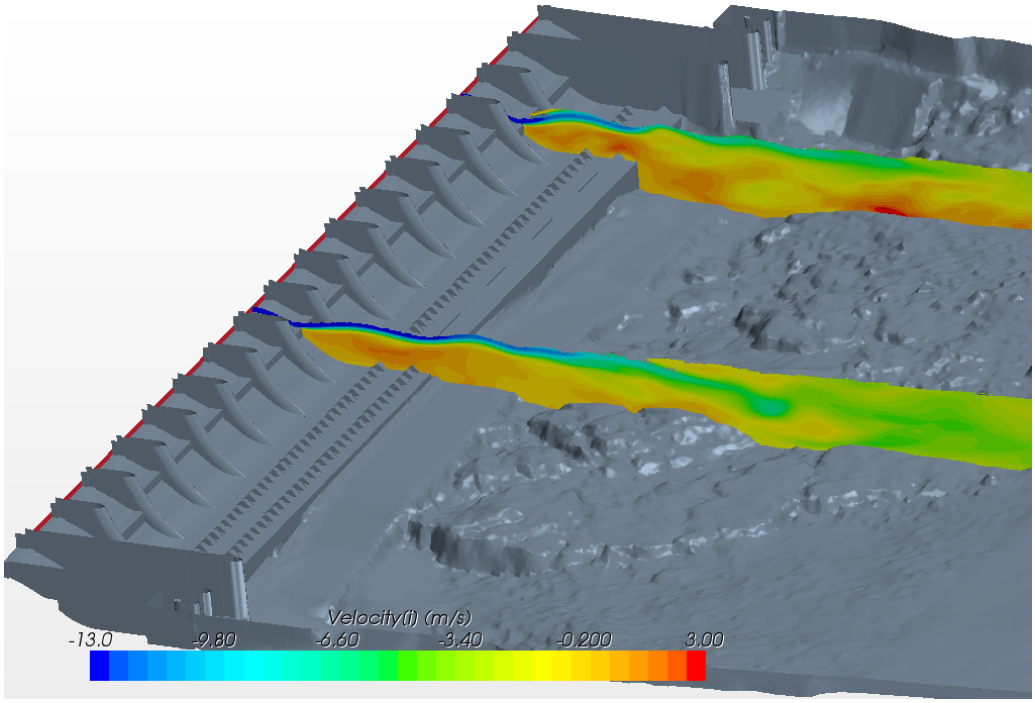

Figure 3.2. Run 1 inflow jet for Bays 9 and 16 with 14-ft and 7-ft elevation deflectors, respectively. Bay 9 was classified as a skimming surface jet, Bay 16 as an unstable surface jump.

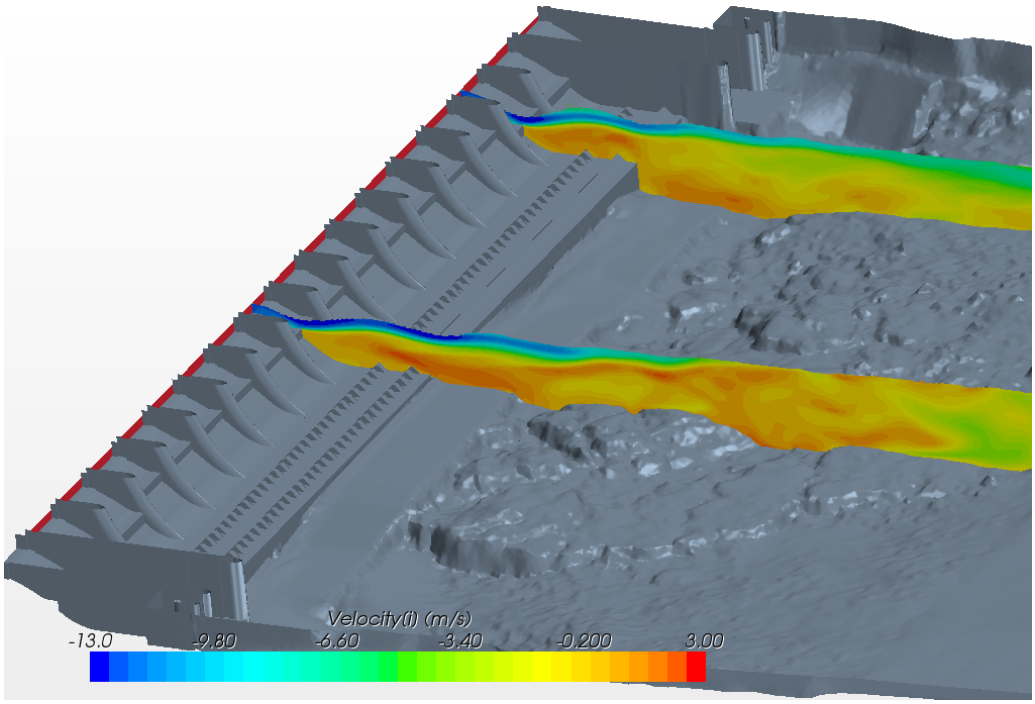

Figure 3.3. Run 3 inflow jet for Bays 9 and 16 with 14-ft and 7-ft elevation deflectors, respectively. Bay 9 was classified as a skimming surface jet, Bay 16 as a surface jet.

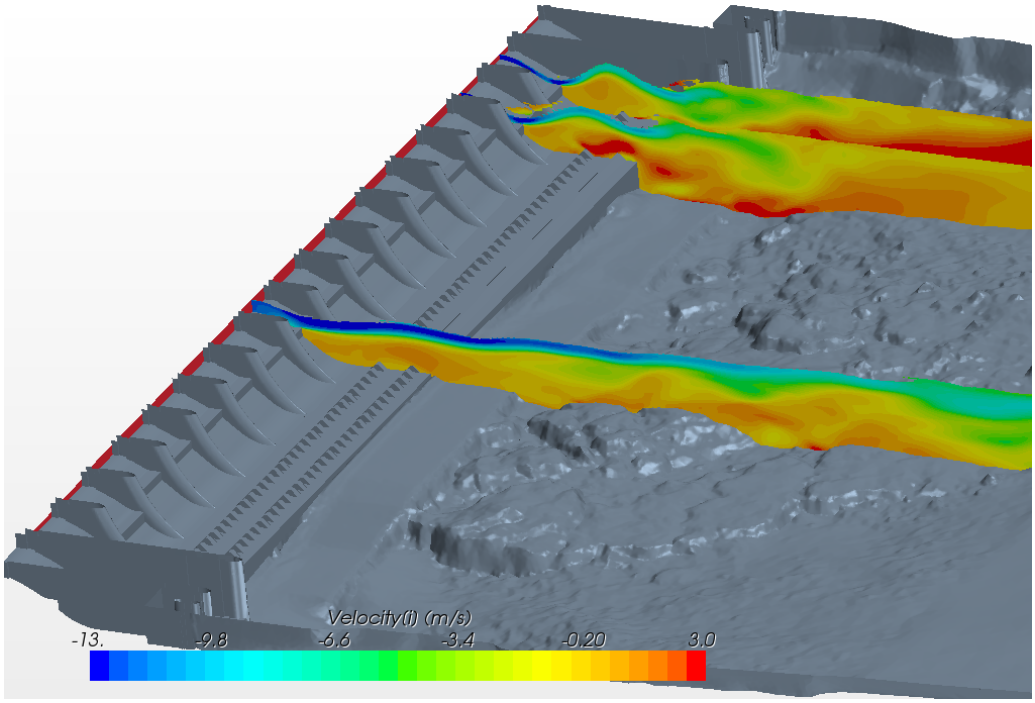

Figure 3.4. Run 4 inflow jets for Bays 9, 16 and 17 with 14-ft, 7-ft, and 7-ft elevation deflectors, respectively. Bay 9 was classified as a skimming surface jet, Bays 16 and 17 as surface jumps.

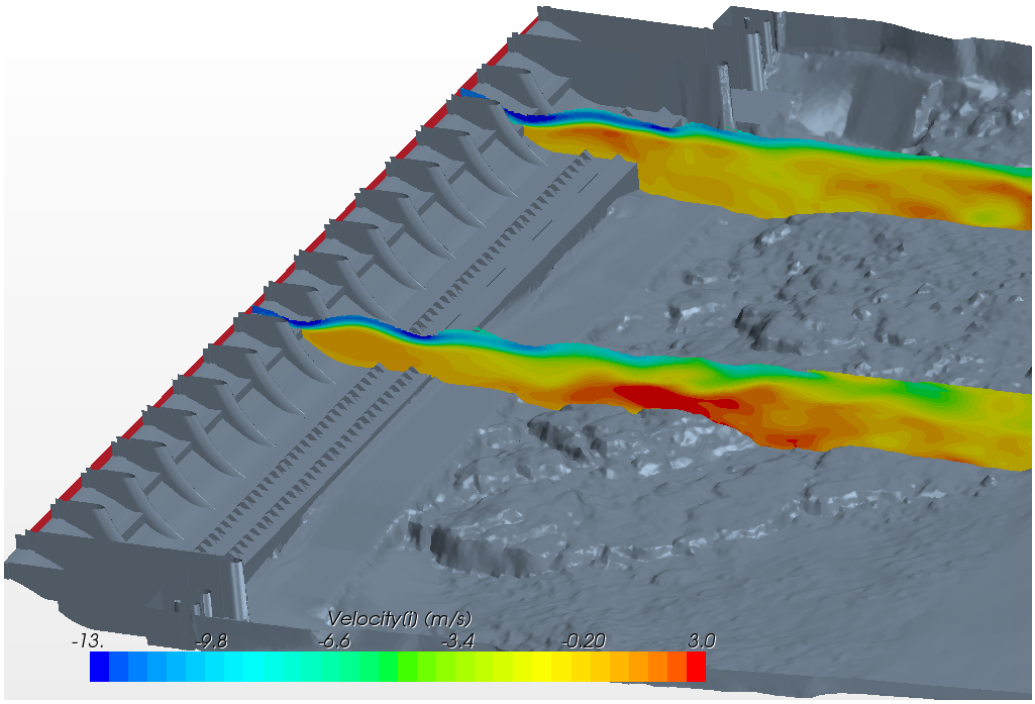

Figure 3.5. Run 6 inflow jet for Bays 9 and 16 with 14-ft and 7-ft elevation deflectors, respectively. Bay 9 was classified as an undulating surface jet, Bay 16 as a surface jet.

3.2 Flow Scenarios

Four spillway discharge scenarios were run. Streamline and water surface elevation plots were created for all runs. The streamlines make the 3D structure of the flow very obvious. Interrogation of the CFD model results showed downstream flows near the water surface and very complex flows lower in the water column for all scenarios.

As one of the CFD model checks, the discharge in kcfs was calculated on the outflow boundary, midway in the model, and at the inflow boundaries. Figure 3.6 shows the model progression for Run 3. Such a check ensures the inflow volume is correct (note there was a slight adjustment for the overall low inflow about iteration 200000) and that the "sloshing" has settled out. This outflow check was done for all simulations.

Figure 3.6. CFD model discharge in kcfs for Run 3. Target discharge was 300 kcfs.

3.2.1 Medium Spill, Flat Pattern (Run 1)

This scenario had a flat spill pattern (about equal discharge through Bays 2 to 17) for a total spillway discharge of 200 kcfs. Based on observations at the prototype, this spill pattern was expected to have no rock movement into the stilling basin.

Streamlines seeded at 9 locations in each bay (3 x 3 array in each bay) are shown in Figure 3.7, top. The streamlines are colored by downstream velocity with warm colors indicating upstream

movement. A very large recirculation zone was present on the north end of the spillway on the Cascade Island shore. This recirculation zone extended about half way across the channel,with the recirculation near the river bottom having a larger extent across the river. There was recirculation on the south end of the spillway, but its lateral extent was much more limited. Streamlines moving upstream were located across the length of the spillway and were as far upstream as the foot of the ogee. Bays with the 14-ft deflectors (4 through 15) had standing waves downstream of the ogee and a submerged jump was modeled at the bays with 7-ft deflectors (Figure 3.7, bottom).

Near-bed flow velocities show that velocity magnitudes exceed 2.5 m/s (8.2 ft/s) in many locations (Figure 3.8). Critical erosion velocity is about 9 ft/s for cobbles(American Society of Civil Engineers 1975). Figure 3.8, lower left includes vectors to show flow direction; the lower right shows the near-bed seeded streamlines. These show the upstream velocities onto the apron, however, the north shore recirculation has a lower velocity area before reaching the apron. On the south shore, there is a very limited area with larger velocities that move upstream onto the apron, although large areas on the north side that have downstream flow just off the apron.

3.2.2 High Spill, Flat Pattern (Run 3)

This scenario had a flat spill pattern (about equal discharge through Bays 2 to 17) for a spillway discharge of 300 kcfs. Based on observations at the prototype, this spill pattern was expected to have rock movement into the stilling basin.

The streamlines (Figure 3.9, top) show that the lateral extent of the northern recirculation cell is more limited along the shoreline, but there is upstream flow near the river bottom from downstream of the concrete back into the stilling basin and to the foot of the ogees across the stilling basin. The upstream velocities are larger than were simulated in Run 1. Figure 3.9 (bottom) shows the modeled water surface elevation. A series of standing waves was produced downstream of the spillway.

Near-bed flow velocities show that velocity magnitudes exceed 2.5 m/s (8.2 ft/s) in many locations (Figure 3.10), although only in limited areas on the apron. Figure 3.10, lower left, includes vectors to show flow direction; the lower right shows the near-bed seeded streamlines. These show continuous areas of upstream velocities onto the apron on both the north and south side of the spillway. On the south shore, the area with upstream velocities in excess of 2.5 m/s is larger than in Run 1 and moves upstream onto the apron. On the north side, there is also a connected "thread" of upstream velocities that move from the edge onto the apron.

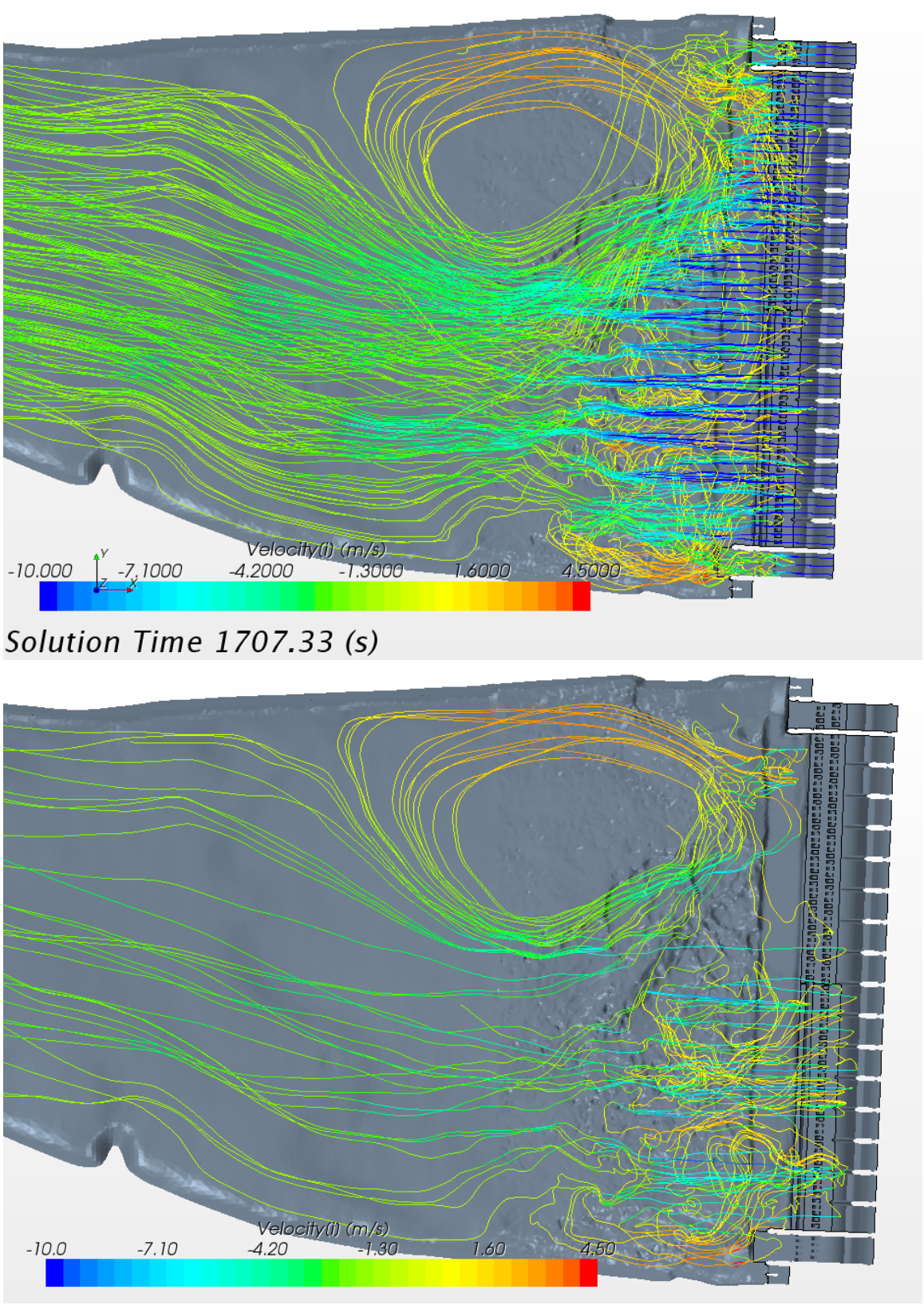

Figure 3.7. Run 1 - 200-kcfs spill discharge streamlines colored by downstream velocity. Top figure shows streamlines seeded in the spillway inlets; bottom figure shows streamlines seeded downstream of the apron 0.5 m above the bed.

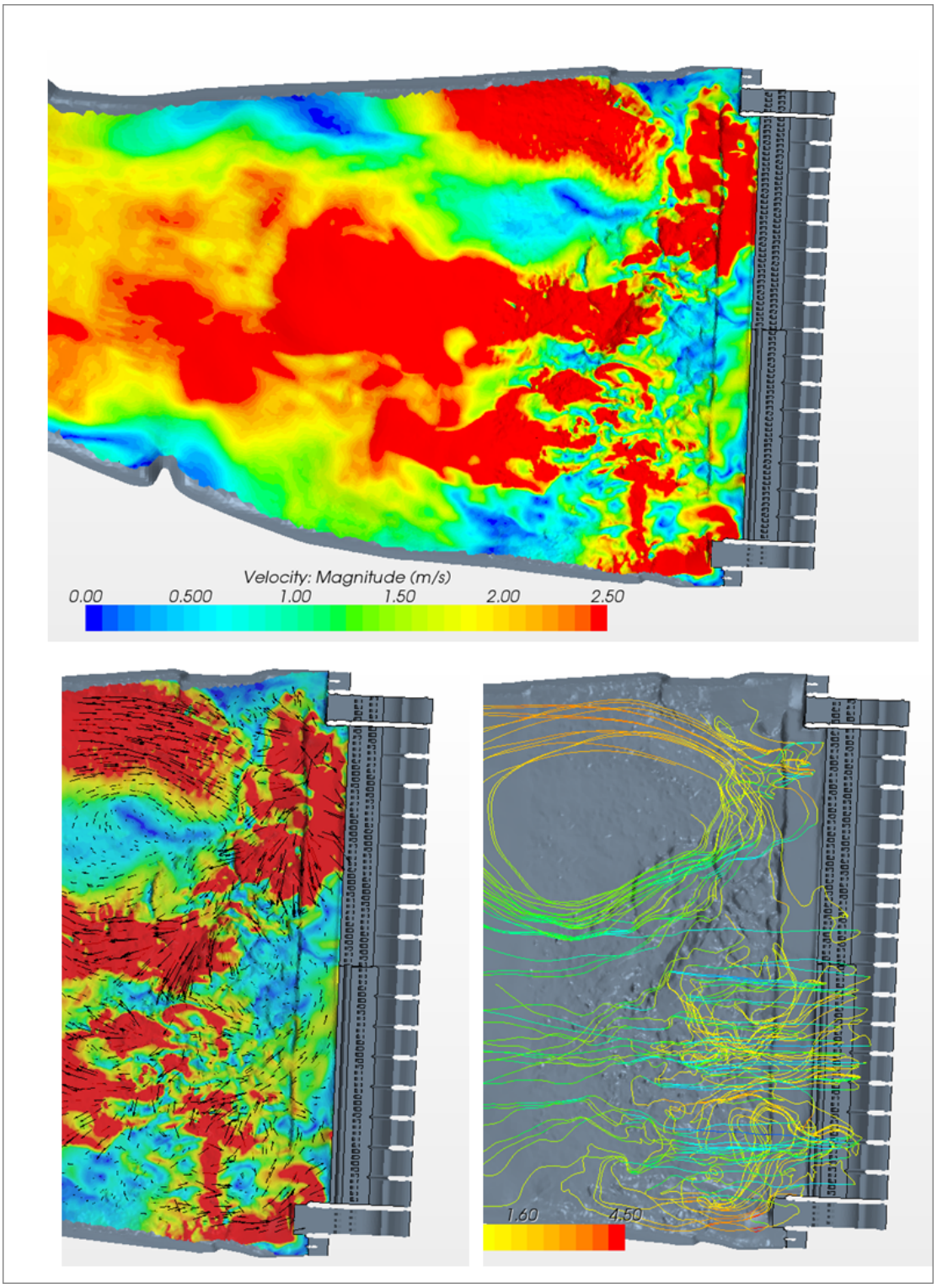

Figure 3.8. Near-bed (0.5 m above) velocities for Run 1. Spill pattern had 200-kcfs spill with a flat spill pattern. Velocity magnitude (top), near-bed velocity with added vectors (bottom left), and streamlines colored by downstream velocity seeded downstream of the apron 0.5 m above the bed (bottom right).

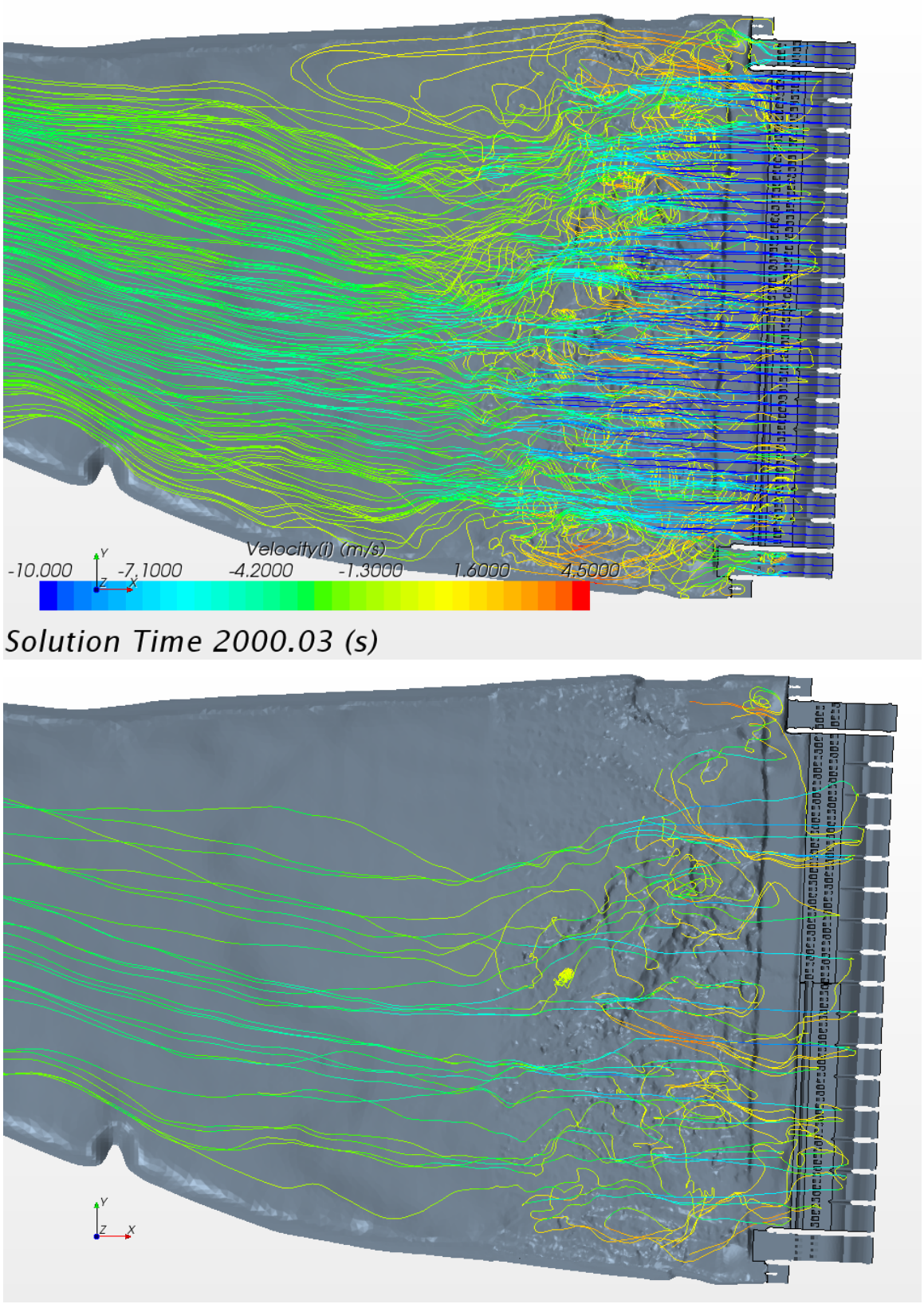

Figure 3.9. Run 3 - 300-kcfs spill discharge streamlines colored by downstream velocity. Top figure shows streamlines seeded in the spillway inlets; bottom figure shows streamlines seeded downstream of the apron 0.5 m above the bed.

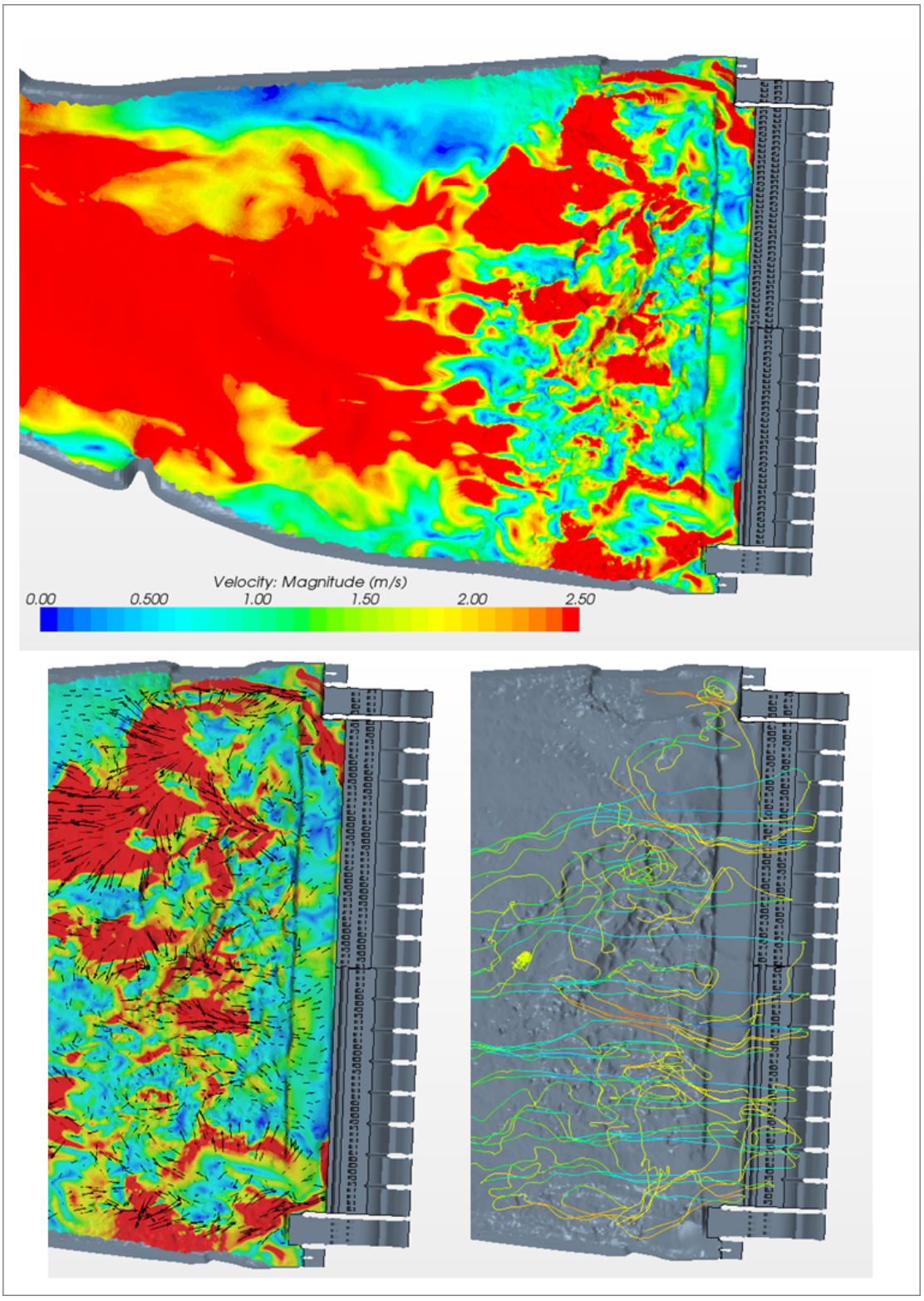

Figure 3.10. Near-bed (0.5 m above) velocities for Run 3. Spill pattern had 300-kcfs spill with a flat spill pattern. Velocity magnitude (top), near-bed velocity with added vectors (bottom left), and streamlines colored by downstream velocity seeded downstream of the apron 0.5 m above the bed (bottom right).

3.2.3 High Spill, Center Maximum Pattern (Run 4)

This scenarios had larger spill volumes through the bays in the center of the spillway. The CFD results showed flow concentrated in the center of the tailrace, with large recirculation cells and large upstream velocities (greater than 4.5 m/s) in places along the shorelines. The area of upstream velocity in excess of 4.5 m/s is much greater than modeled in any other scenario. The recirculation zone on the north side extended underneath the spillway flow as far over as Bay 7. On the south side, the recirculation extended over in front of Bay 13 underneath the spillway flows.

Near-bed flow velocities show that velocity magnitudes exceed 2.5 m/s (8.2 ft/s) in many locations (Figure 3.12), with large areas of connected upstream flow onto the apron. Figure 3.12, lower left, includes vectors to show flow direction; the lower right shows the near-bed seeded streamlines. These show large continuous areas of upstream velocities onto the apron on both the north and south side of the spillway with a much larger "contributing" area downstream.

3.2.4 High Spill, Bimodal Pattern (Run 6)

Run 6 had the spill distributed in a bimodal pattern with lower discharges in the center and on the north and south ends of the spillway. This inflow pattern results in much upstream flow lower in the water column. There is a larger number of streamlines seeded under the spillway gates that return upstream into the stilling basin and the base of the ogees than for either the flat pattern (Run 3) or the center loaded pattern (Run 4).

Near-bed flow velocities are very similar to Run 3 (Figure 3.14), although upstream flow onto the apron is even more limited and discontinuous that Run 3. Figure 3.14, lower left, includes vectors to show flow direction; the lower right shows the near-bed seeded streamlines.

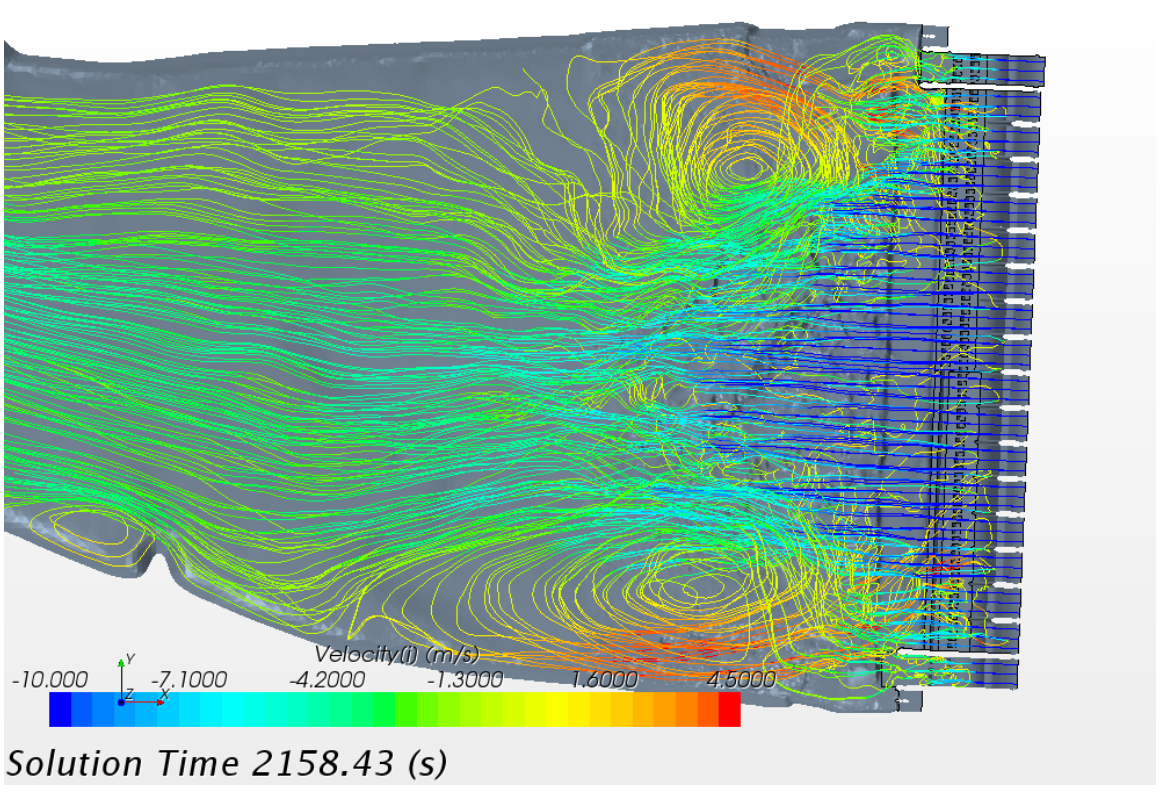

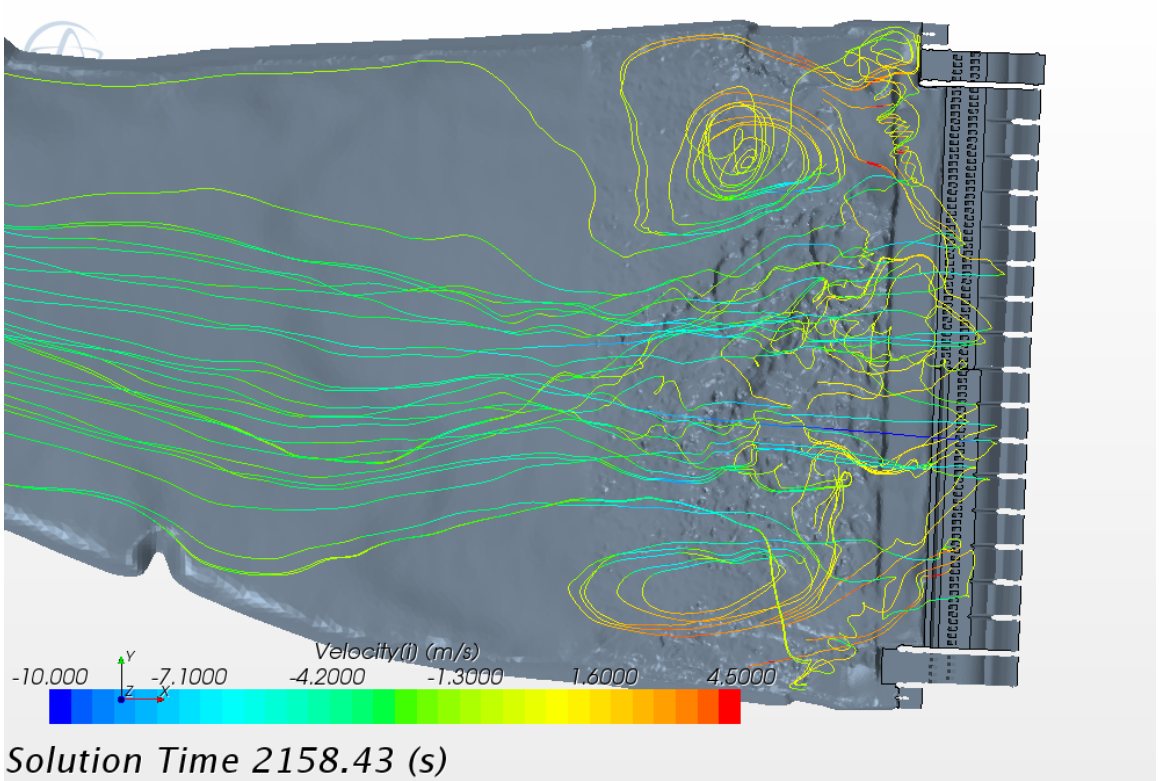

Figure 3.11. Run 4 - 300-kcfs spill discharge streamlines colored by downstream velocity. Top figure shows streamlines seeded in the spillway inlets; bottom figure shows streamlines seeded downstream of the apron 0.5 m above the bed.

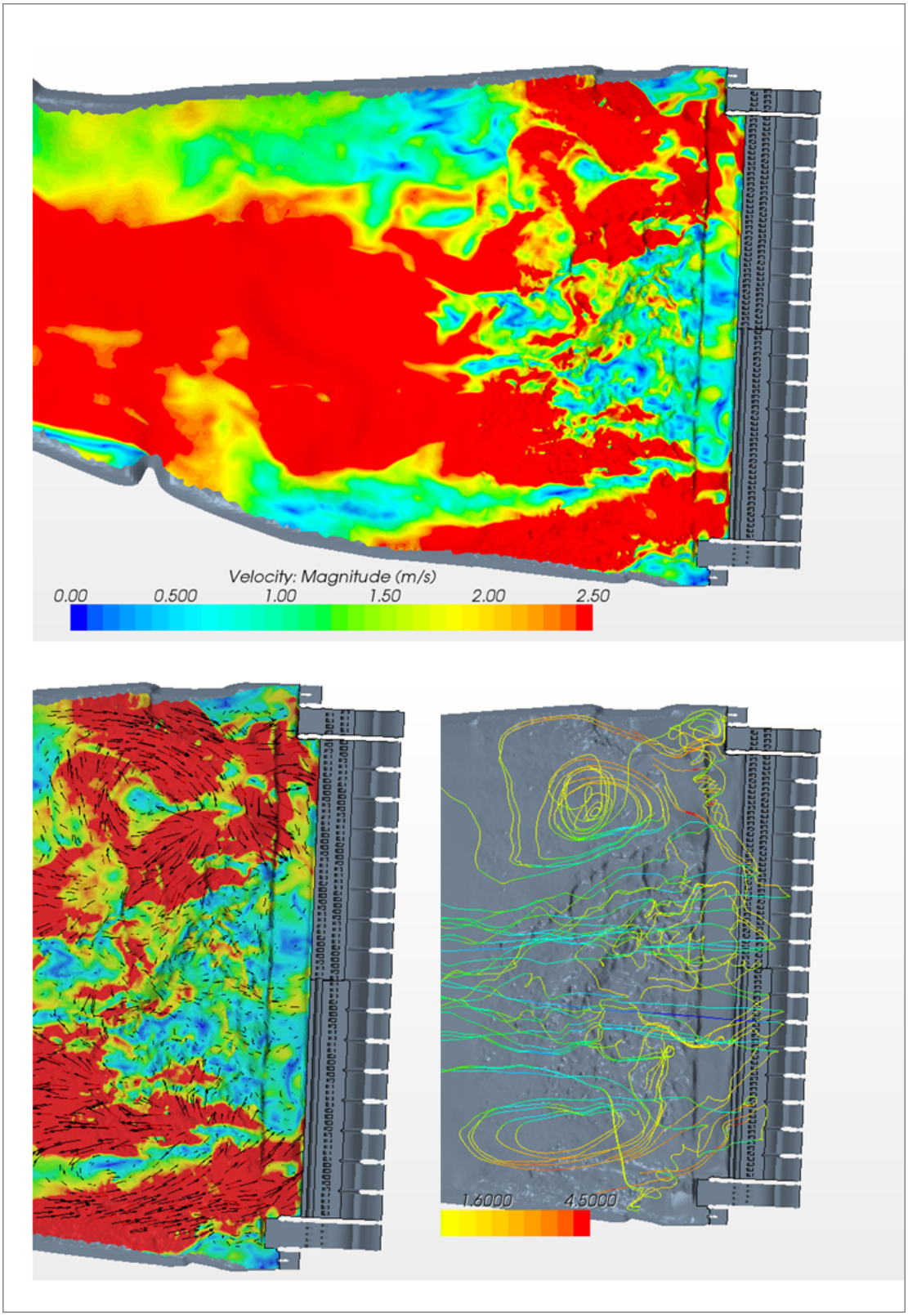

Figure 3.12. Near-bed (0.5 m above) velocities for Run 4. Spill pattern had 300-kcfs spill in larger discharges in the center of the spillway. Velocity magnitude (top), near-bed velocity with added vectors (bottom left), and streamlines colored by downstream velocity seeded downstream of the apron 0.5 m above the bed (bottom right).

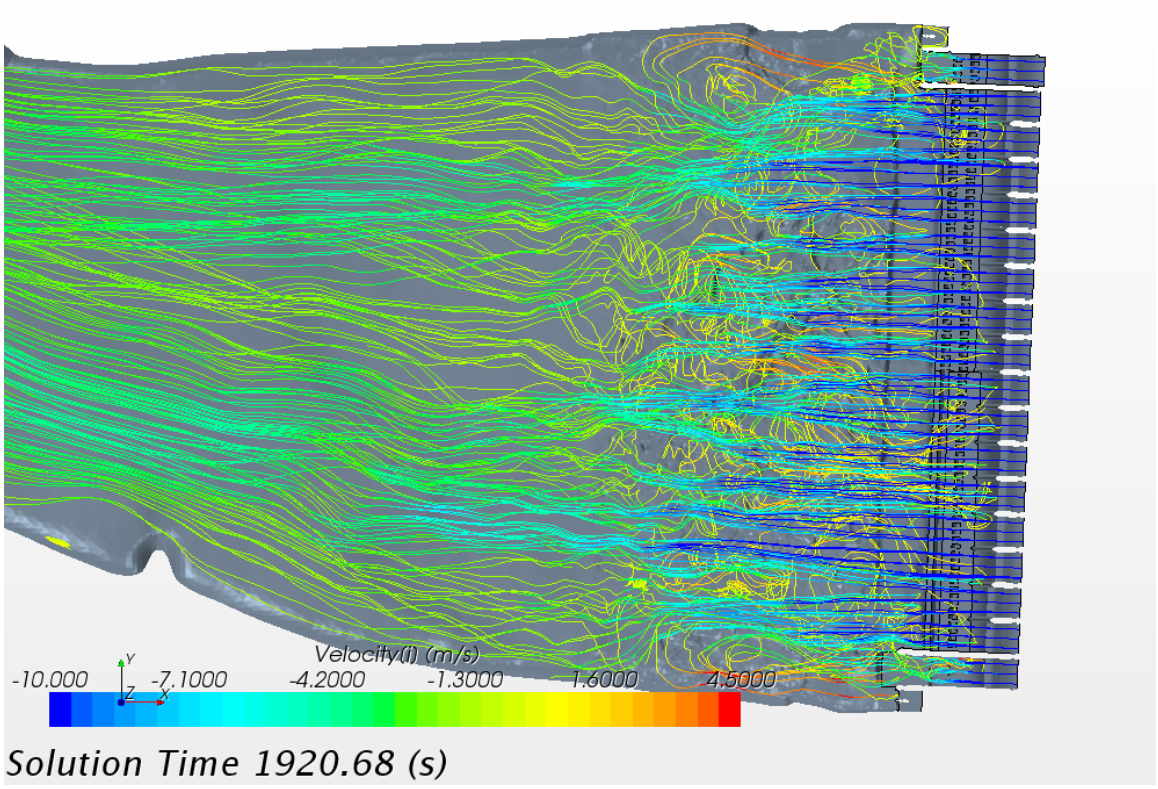

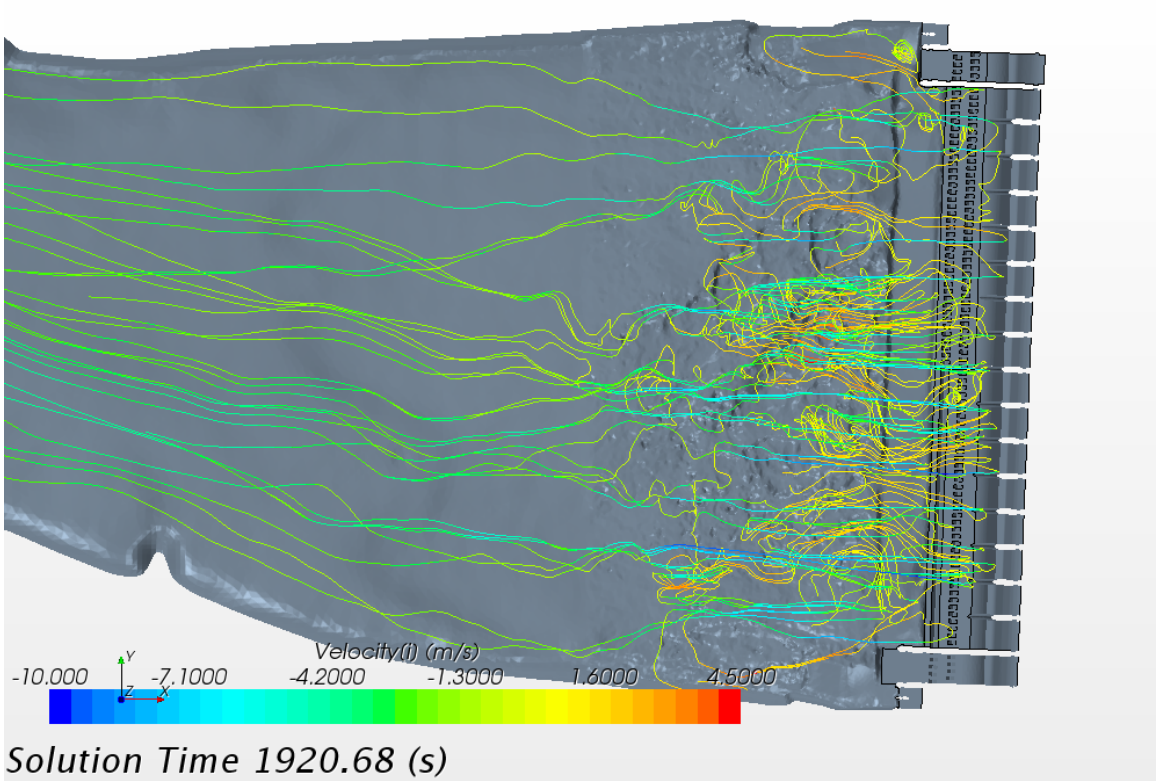

Figure 3.13. Run 6 - 300-kcfs spill discharge streamlines colored by downstream velocity. Top figure shows streamlines seeded in the spillway inlets; bottom figure shows streamlines seeded downstream of the apron 0.5 m above the bed.

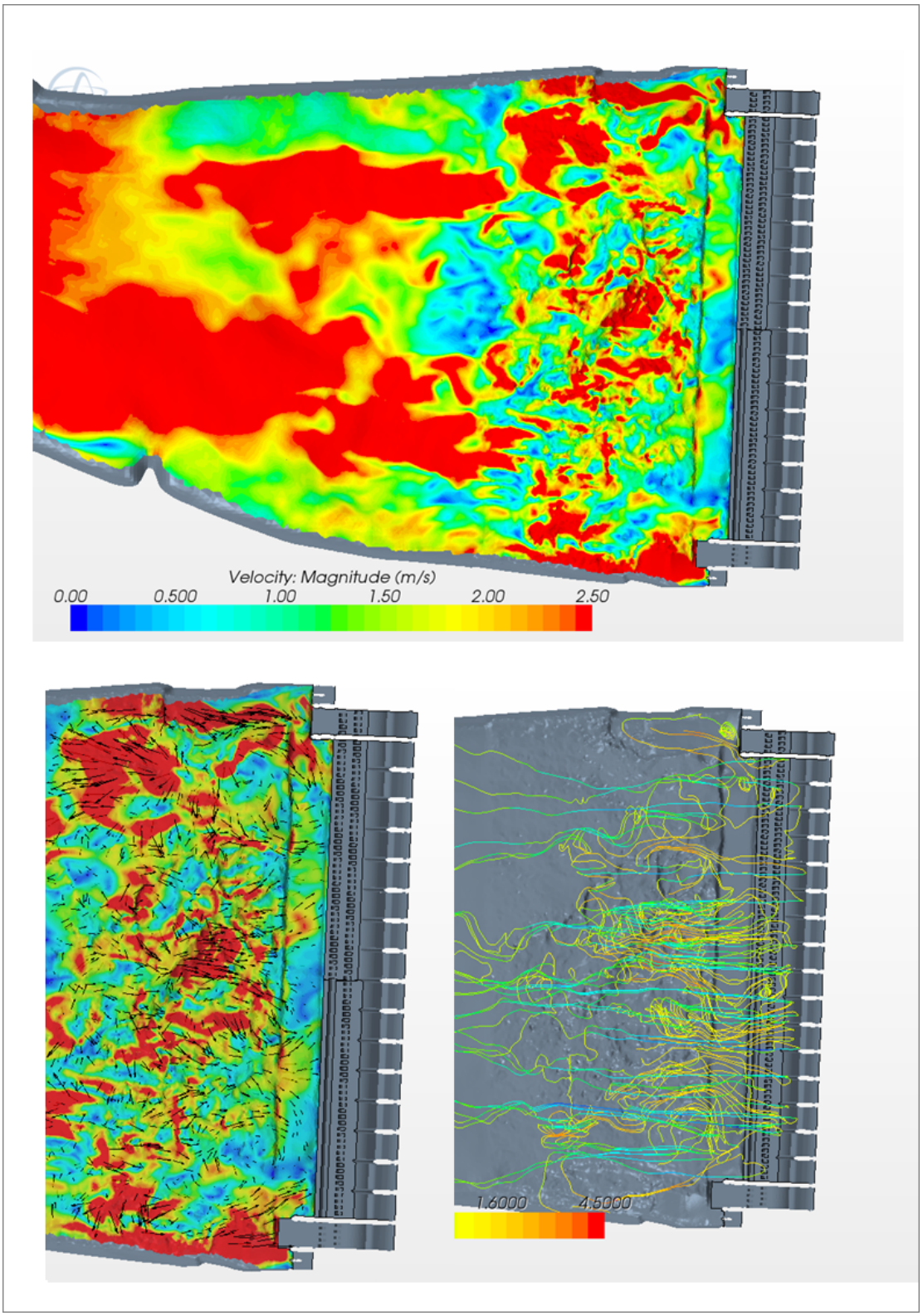

Figure 3.14. Near-bed (0.5 m above) velocities for Run 6. Spill pattern had 300-kcfs spill in larger discharges in the center of the spillway. Velocity magnitude (top), near-bed velocity with added vectors (bottom left), and streamlines colored by downstream velocity seeded downstream of the apron 0.5 m above the bed (bottom right).

3.2.5 Water Surface Elevation

Water surface elevation plots are useful for seeing the overall distribution of the discharge and certain features such as the location of standing waves. Figure 3.15 shows the water surface elevation for similar spill patterns (a flat spill pattern) for 200-kcfs (top) and 300-kcfs (bottom) discharges. The lower discharge has a lower tailwater elevation and hence overall lower water surface. With the lower discharge volume, however, a large recirculation zone was modeled on the north side. This feature is evident in the plot as the lower elevation zone on the north shore and is visible in the streamlines shown in Figure 3.7. There were also standing waves downstream of the ogees and a much different features in Bays 1 and 18 which have confining walls on both sides. The difference between the deflector elevations is particularly visible on the 300-kcfs run. Bays 1, 2, 3, 16, 17, and 18 have 7-ft deflectors.

The overall water surface elevation was very similar for Run 4 and Run 6 (Figure 3.16. These models had the same spillway discharge, but very different spill patterns. Run 4 had the largest discharge volumes in the middle; Run 6 had a bimodal distribution with lower discharges in the middle and on the edges. Both had a series of standing waves downstream of the ogee with more bands of waves in the center of the Run 4 channel, but more the waves were more evenly distributed for the bimodal distribution of Run 6. Run 6 was also similar to Run 3, although the standing waves were distributed further toward the shore. This resulted from the smaller shoreline recirculation zones modeled in Run 6 than in Run 3.

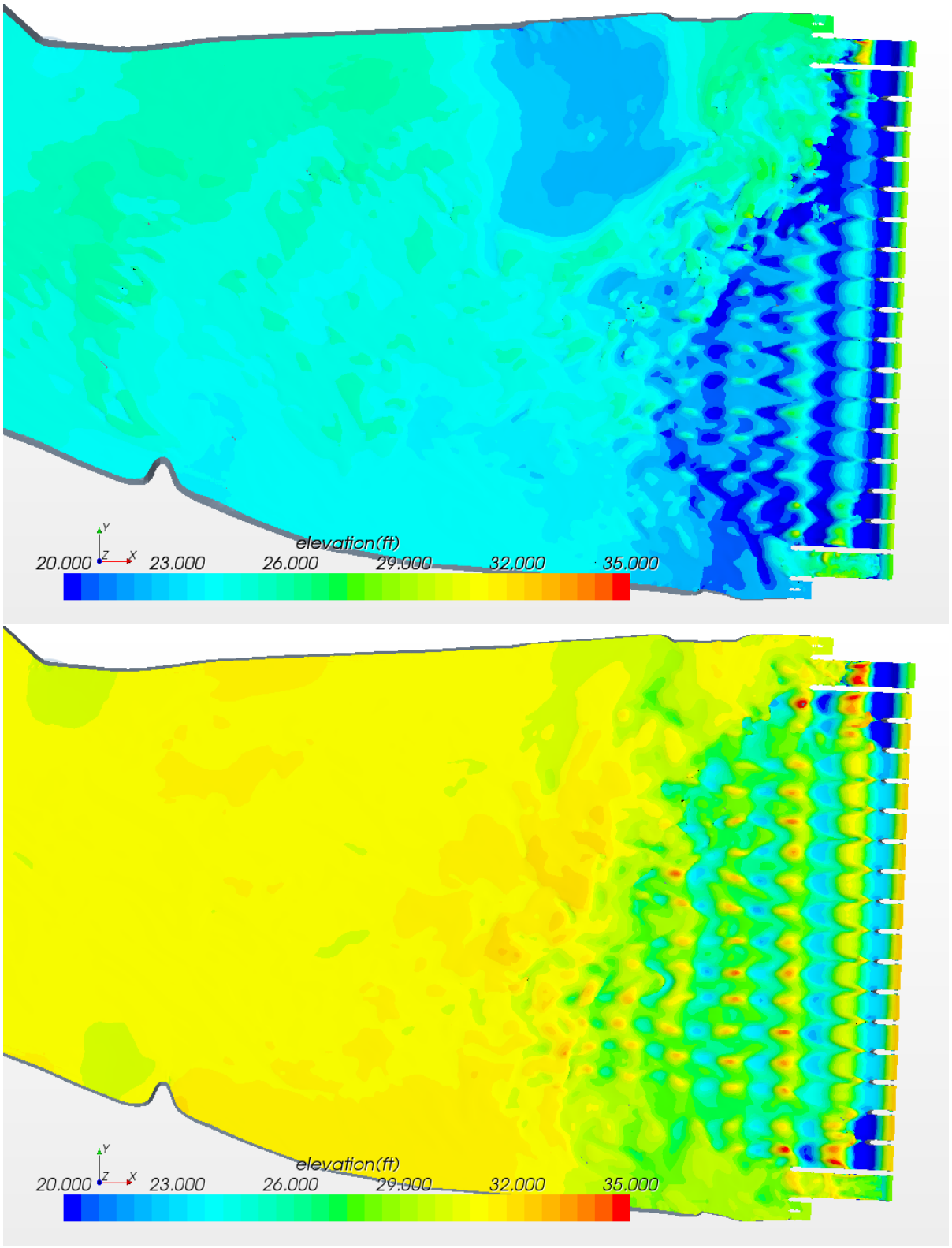

Figure 3.15. Water surface elevation of Run 1 (200-kcfs spill discharge, top) and Run 3 (300-kcfs spill discharge, bottom).

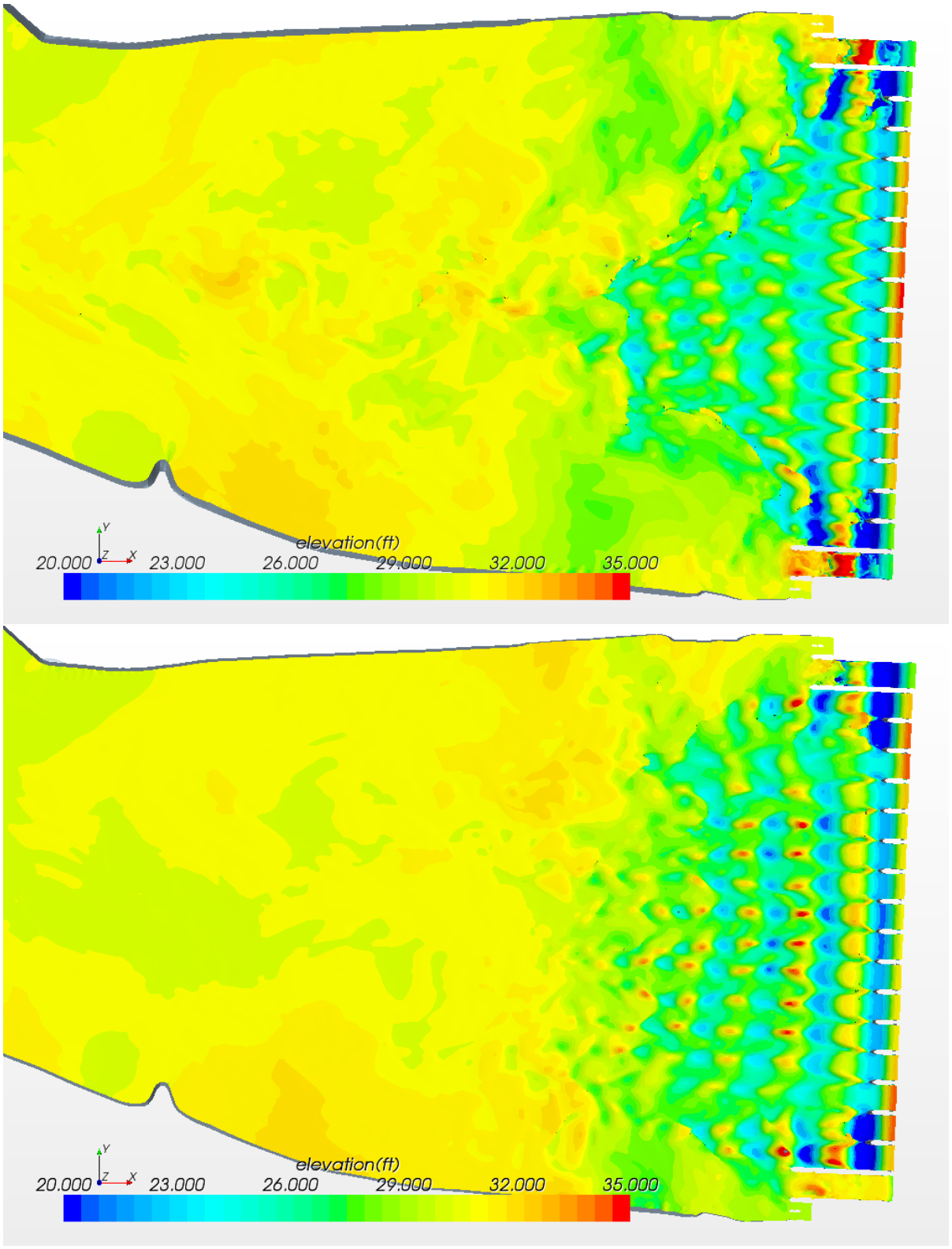

Figure 3.16. Water surface elevation of Run 4 (top) and Run 6 (bottom).

3.3 Near-Bed Particle Tracking and Potential Rock Movement

The streamlines discussed in the above sections describe the flows originating in the spillway basins. In addition to understanding the general hydraulics of the tailrace, additional information related to how rock may move from downstream of the apron into the stilling basin is needed.

Plots of vertical slices of the downstream velocity (e.g., Figure 3.3), show that there are upstream velocities near the river bottom. To characterize the flows near the river bed, it was necessary to use a different approach to track the flows near the river bed.

Figures 3.17, 3.18, and 3.19 show the initial location of the spherical particles that represented rock material, as well as the end locations after 300 seconds of physical time. In all instances, this time span was enough to allow for either particle settling or periodic motion contained within local bathymetry. In Figure 3.17 (bottom), the particles tracked under a single time step flow solution have more widespread final locations in comparison to the transient flow case. In the latter, particles tend to move nearer to the apron. However, the overall tendency to travel towards the stilling basing, in a direction opposite to the mean flow, is manifest regardless of the temporal flow formulation. The test of seeding locations under transient flow (Figures 3.18 and 3.19) further confirmed the previously described tendency, with most particles clustering on the step to the stilling basin near the initial rectangular array (Figure 3.18), whereas those in an initial lineal arrangement remain on the apron at the end of the simulation time (Figure 3.19). Furthermore, the latter configuration indicates that there is limited particle movement in the transverse direction as each distinctive settling cluster is composed of particles initially placed in the neighboring arrangements (circles in Figure 3.19). Animations of particle movement described above were provided to CENWP.

A limitation of this qualitative modeling approach was that the particles did not travel upstream into the stilling basin, where significant amounts of rock material has been observed and removed. Nevertheless, the current preliminary results point to potential improvements on the modeling techniques to better represent the movement of rock material of large and varying dimensions. The use of actual material densities will require much longer simulation times than those currently in use. Furthermore, environmental flows are turbulent in nature, a condition that is known to promote enhanced momentum transfer to material particles and hence sediment movement. Thus, the surging material motion that takes place at longer time spans can better be represented with turbulent modeling schemes such as detached eddy simulations (DES). In addition, a formulation for the lift force acting on rock material in natural flows is likely to better describe the driving mechanism for particles moving to the stilling basin, instead of the implementation of the lift force in this work which was derived from work with small-sized particles (millimeters). Lastly, the large volumes of rocks removed from the spillway stilling basin (Figure 1.3) suggest that the particle-to-particle interactions are significant in the course of the material buildup and cannot be considered negligible. This issue can be addressed with a modeling approach in which particle interactions can be defined, such as the discrete element method (DEM).

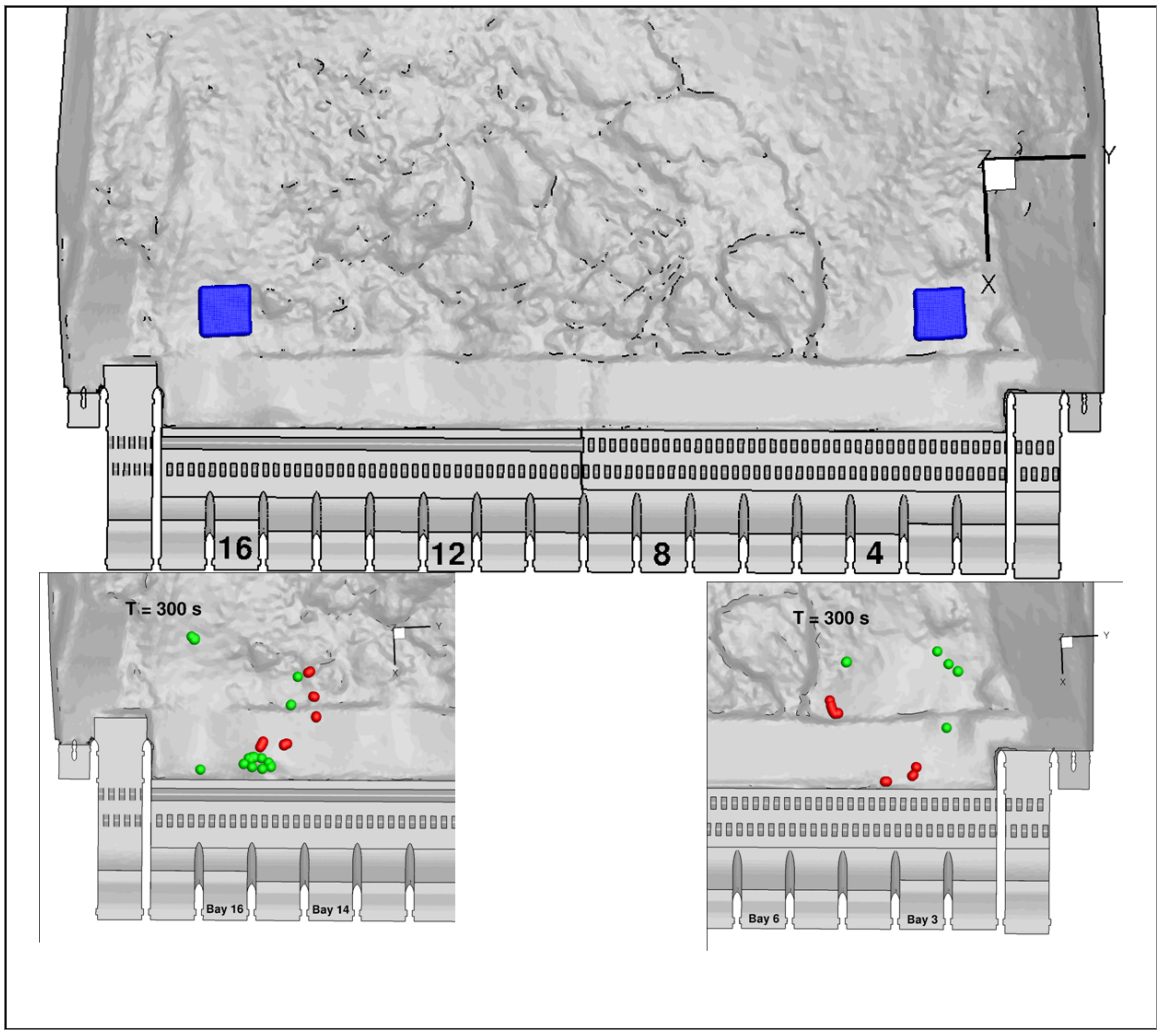

Figure 3.17. The initial seeding of Lagrangian particles (top) resulted in distinctive locations after 300 seconds based on whether the flow solution was from a single time step (green) or transient (red) (bottom).

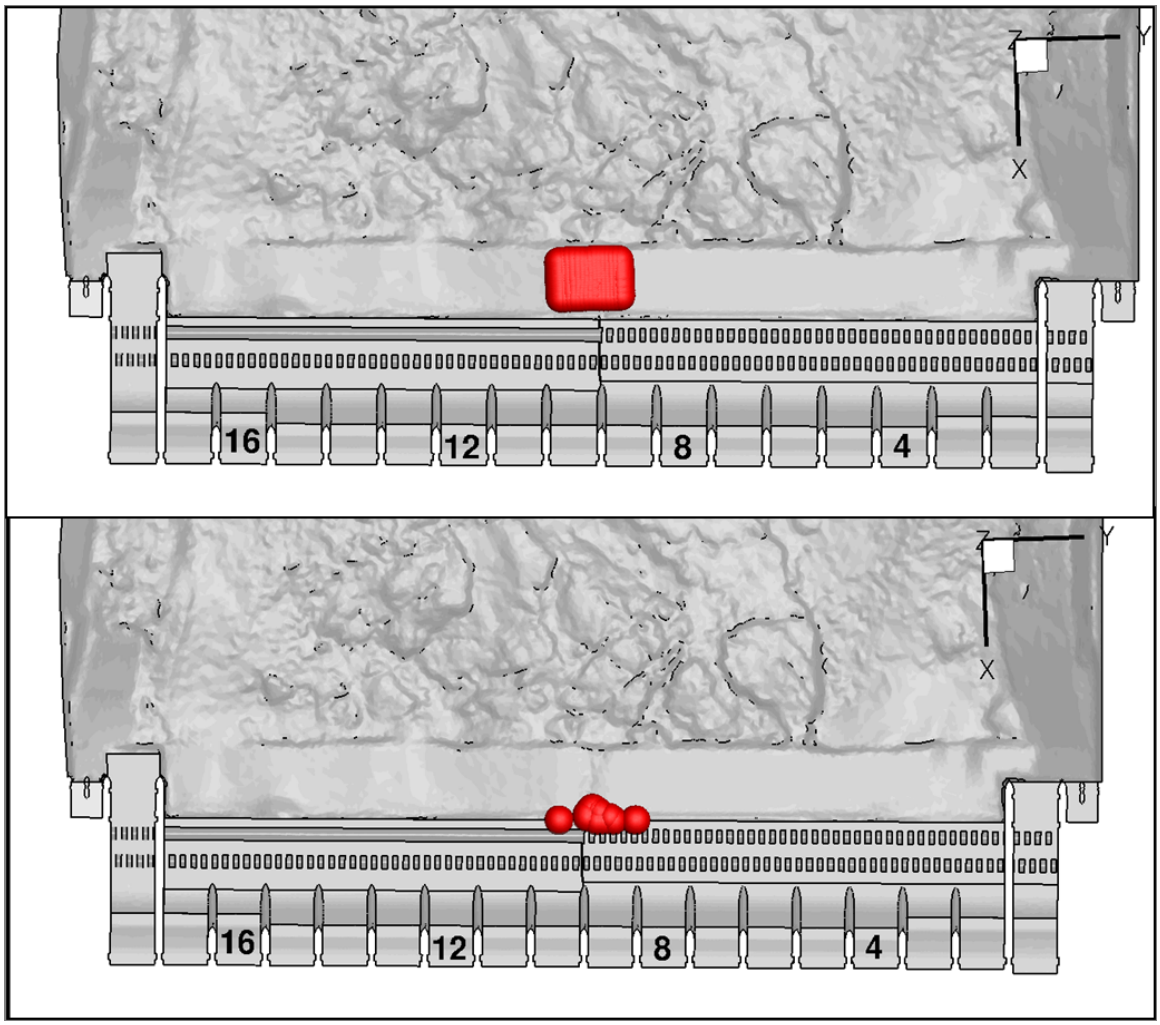

Figure 3.18. Initial (top) and end (bottom) locations of Lagrangian particles seeded downstream from the baffle blocks in a rectangular arrangement.

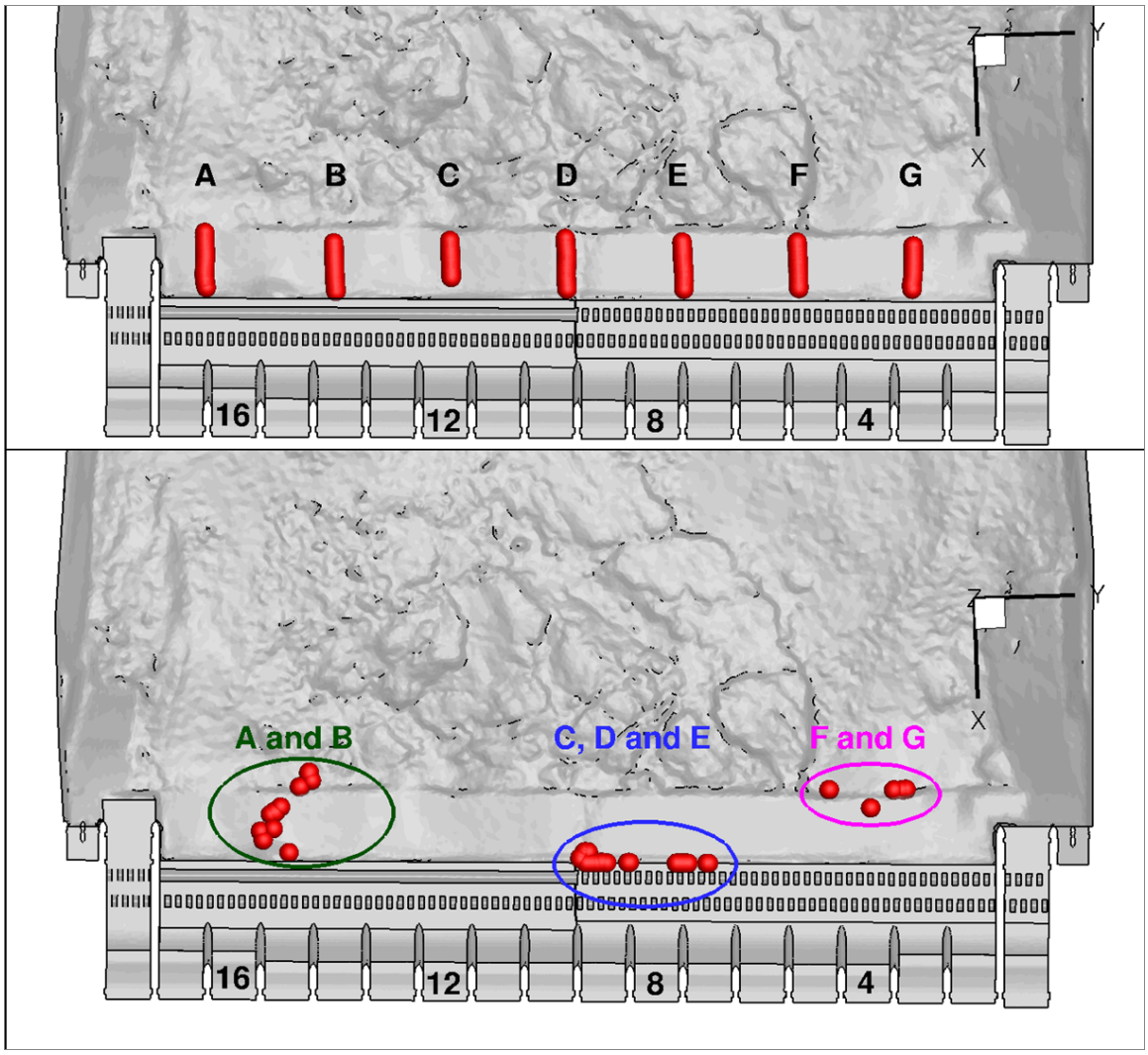

Figure 3.19. Initial (top) and end (bottom) locations of Lagrangian particles seeded along lines on the apron downstream of the stilling basin.

4.0 Conclusions

A free-surface CFD model of the Bonneville spillway tailrace was developed and applied for four discharge scenarios. These scenarios looked at the impact of discharge volume and distribution on tailrace hydraulics. The simulation results showed that areas of upstream flow existed near the river bed downstream of the apron, on the apron, and within the stilling basin for all discharges. For spill discharges of 300 kcfs, the cross-stream and downstream extent of the recirculation zones along Cascade and Bradford islands was very dependent on the spill pattern. The center-loaded pattern had much larger recirculation zones than the flat or bimodal pattern. The lower discharge (200 kcfs) with a flat pattern had a very large recirculation zone that extended halfway across the channel near the river bed.

A single scenario (300 kcfs in a relatively flat spill pattern) was further interrogated using Lagrangian particle tracking. The tracked particles (with size and mass) showed the upstream movement of sediments onto the concrete apron and against the vertical wall between the apron and the stilling basin from seed locations downstream of the apron and on the apron.

Future work should include the development of a more realistic representation of the lift force on the particles as well as particle interactions.

5.0 References

ADAPCO, Computational Dynamics Limited. 2012. *User Guide, STAR-CCM+ Version 7.02.11*. CD-adapco, http://www.cd-adapco.com.

American Society of Civil Engineers. 1975. *Sedimentation Engineering*.

Ecauriaza C and F Sotiropoulos. 2011. "Lagrangian model of bed-load transport in turbulent junction flows." *Journal of Fluid Mechanics* 666:36–76.

Rakowski C, J Serkowski, M Richmond, and W Perkins. 2010. *Computational Fluid Dynamics Modeling of the Bonneville Project: Tailrace Spill Patterns for Low Flows and Corner Collector Smolt Egress*. PNNL-20056, Pacific Northwest National Laboratory, Richland, Washington.

Pacific Northwest
NATIONAL LABORATORY

Proudly Operated by **Battelle** *Since 1965*

U.S. DEPARTMENT OF
ENERGY

902 Battelle Boulevard
P.O. Box 999
Richland, WA 99352
1-888-375-PNNL (7665)
www.pnnl.gov